THESIS

SOME CHARACTERISTICS OF TURBULENCE IN THE LOWER 200 FEET OF THE ATMOSPHERE

Submitted by

Borislava Stankov

In partial fulfillment of the requirements

for the Degree of Master of Science

Colorado State University

Fort Collins, Colorado

August 1970

CER70-71BS14

(also: CET70-71BS9)

ABSTRACT OF THESIS

SOME CHARACTERISTICS OF TURBULENCE IN THE
LOWER 200 FEET OF THE ATMOSPHERE

The small scale structure of turbulence and the variation of the longitudinal turbulent component with stability are discussed. The analog computing technique used in the calculations is presented. It is shown that the spectrum distribution of the turbulent fluctuations follows the -5/3 law of Kolmogorov. The intermittency factor, γ , defined by Townsend is computed for different frequencies of the original signal. The flatness factor for the present data shows good agreement with the previous investigations. The Richardson number is computed in the layer between 200 and 20 feet for each fifteen minutes during a 24 hour period. Turbulent macro-scales during the same period of time were computed and discussed in relation to stability.

ACKNOWLEDGMENTS

The author wishes to express her sincere gratitude to her advisors, Professors Virgil A. Sandborn and Elmar R. Reiter, for their guidance and valuable advice during this research. Appreciation is also expressed to Dr. William Marlatt for taking time to read and comment on the manuscript.

The author also wishes to express appreciation for the help in reducing the data to Mr. David Pickelner and Mr. Lewis Huff. Special thanks are given to Mr. Peter F. Lester for a valuable discussion on the problems of turbulence.

To those who assisted in typing and printing this manuscript the author extends her gratitude.

This research was performed under National Aeronautics and Space Administration (NASA) Contract No. NAS8-21049, Control No. DCN 1-7-75-20042(IF).

TABLE OF CONTENTS

LIST OF TABLES

LIST OF FIGURES

LIST OF FIGURES - Continued

LIST OF SYMBOLS

Symbol	Definition
U	mean wind speed
V	linear speed of the cup centers
a,b,c	constants
e_o	operational amplifier gains
R_o, R_1	resistance in the circuit
R_H	hot-wire resistance
I	current through the hot wire
$R(t)$	time autocorrelation function
D	total integration time
$u(t)$	velocity signal at the time t
$u(t+\tau)$	velocity signal at the time $t + \tau$
τ	delay time
τ_o	time constant
e	the hot-wire voltage fluctuation
E	mean voltage
$\overline{T}$	mean temperature
t'	temperature fluctuation
$F(f)$	one-dimensional spectrum in terms of frequency
f	frequency in CPS
k	wave number
$F'(k)$	one-dimensional spectrum function in terms of wave number
$\overline{u^2}$	root mean of wave of longitudinal
ϵ	the rate of dissipation of turbulent kinetic energy
γ	intermittency factor
ν	kinematic viscosity

LIST OF SYMBOLS - Continued

Symbol	Definition
ℓ	signal amplitude
F.F	flatness factor
P(e)	probability density function
A	constant
Ri	Richardson number
K_H	eddy diffusivity
K_M	eddy viscosity
$\partial T/\partial z$	temperature lapse rate
Γ	dry adiabatic lapse rate
$\partial \overline{u}/\partial z$	vertical wind shear
R(x)	space correlation coefficient
L	macroscale of turbulence
λ	microscale of turbulence
E(k)	three-dimensional spectrum function
B	band width

INTRODUCTION

In order to understand the structure of physical processes in the layer of air nearest to the ground, it is necessary to examine and interpret highly accurate observations made in this layer. This implies a detailed knowledge about the air motion and temperature changes near the ground. The flow in the boundary layer is usually turbulent and as a consequence many of the characteristic properties on which much of life depends are due to turbulence. Processes such as heat transfer from ground to air, the exchange of carbon dioxide between plant and animal life, the scattering of pollen, the cycle of water from the earth, seas and rivers to the air and back again, propagation of waves and diffusion are all strongly affected by turbulence.

The most frequently used theory in describing turbulent motion is based on a statistical approach. Very important characteristics which describe the turbulent motion, such as correlation functions, spectrum, and scale of turbulence, can be inferred using statistical description. The theory is based on the concept of isotropy, or at least local isotropy (Taylor, 1921; Richardson, 1920; Kolmogorov, 1941). In the atmospheric boundary layer isotropy is not achieved. Still, it is possible to use the concepts of the statistical theory of turbulence in the atmosphere, provided that the scale of motion is less than the height above the ground or less than the distance to the nearest inversion (Lumley and Panofsky, 1964). In general anisotropy decreases with increasing frequency, but the decrease is very gradual. Stewart (1969) discussed the ways of separating waves (the large scale motion) from turbulence and concludes that isotropy is not a good enough criterion.

Another property of small scale turbulence is its intermittent nature. It has received a great deal of attention in recent years for atmospheric problems. The phenomenon of intermittency is not a new concept to fluid dynamicists. Corrsin (1943) noted that a hot-wire probe placed near the sharp interface between turbulent and non-turbulent regions showed a characteristically intermittent signal. Townsend (1948) verified Kolmogorov's (1941) theory of local isotropy in the turbulent wake behind a cylinder, but also found that the flow was intermittent. He proposed the intermittency factor γ . Batchelor (1953) states that there is an uneven spatial distribution of energy associated with large wave number components of turbulence. This energy has a great tendency to occur in confined regions of space. Sandborn (1959), Finn and Sandborn (1964), Baldwin and Sandborn (1968), Kuo (1970) and others have pursued laboratory investigation. Bean, et al. (1969)* gave a report on the intermittent nature of turbulence in the atmosphere. They identified two different types of intermittency. In the first one the phenomenon occurs sporadically in time or space and in the second case the boundaries separating different flow regimes are irregular thereby producing local intermittency.

The present study attempts to describe some of the turbulence characteristics mentioned above in the atmospheric boundary layer. Using high response hot-wire anemometers, two sets of wind data were obtained at different levels in the lowest 200 feet of the atmosphere. Turbulence characteristics, such as spectra correlations, scales, and

---

* Proceedings on Spectra of Meteorological Variables, Stockholm, June 9-19, 1969.

intermittency factor obtained from the wind fluctuation measurements with the high response anemometers are of great importance in understanding the problems of atmospheric turbulence. These characteristics were computed based on the statistical theory of turbulence and using the concept of local isotropy.

EXPERIMENTAL STUDY

Field Station

The Colorado State University Meteorological Tower was erected in a shallow valley formed by the St. Vrain Creek and the South Platte River (Figures 1 and 2). The tower was equipped with Climet's cup anemometers mounted at a height of approximately 10 ft, 110 ft, and 200 ft above the ground, and with temperature sensors manufactured by the Winsco Company, and mounted at 205 ft, 22 ft, and -.95 ft. The Colorado State University hot-wire anemometers were mounted at different levels according to the purpose of the experiment. For the present study two sets of data were collected. On May 13, 1967 four hot-wire anemometers were mounted at 20 ft, 65 ft, 110 ft and 155 ft above the ground. The second set of data was taken on May 9-10, 1968 and the four hot-wire anemometers were mounted on a 6 meter boom at the 200 ft level. As the direction of wind changed the boom was rotated so that it faced into the wind.

Measurements

A cup anemometer is a transducer that employs fluid drag as a means of measuring flow velocity (Sandborn, Metrology of Fluid Mechanics). The instrument makes use of the fact that drag is a function of Reynolds number. The inside of the hemisphere gives a drag roughly that of a flat surface perpendicular to the flow. The drag of the flat plate or disk is greater than that of the outside hemisphere. Thus, the cup anemometer will rotate in a wind. The linear speed of the cup centers, V , is related to the wind speed, U , by a series relation

$$U = a + bV + cV^2 + \ldots\ldots \qquad (1)$$

in which a , b and c are constants. With Climet's instrument c and higher coefficients are zero, so the speed of cup rotation is a linear relation with the wind speed over the total range. This instrument is used to measure the mean wind speed since it does not have a fast enough response to measure the wind fluctuations. Mean wind speeds were recorded inside the instrumentation van (Figure 3), for each level.

In order to measure the turbulent fluctuations of the flow it is desirable to choose a measuring device with little or no bulk to change as the velocity changes. Thus, the hot wire which is extremely small, of the order of 10^{-4} in. in diameter, is the best device. The hot-wire anemometer is a temperature-resistance transducer. The wire is heated electrically by Joulean heating and when put in the fluid flow it's temperature varies (Sandborn, Measurements in Fluid Mechanics). A measure of heat transfer from the wire to the flow can then be related to fluid properties such as temperature, density and fluid velocity. The hot wire measures the instantaneous variations of turbulent flow.

Both experimental and analytical results verify that the step response of a hot wire under constant current operation is very closely approximated by a single exponential function with a time constant of τ_o (C. L. Finn and V. A. Sandborn, 1967, The Design of a Constant Temperature Hot-Wire Anemometer).

As shown in Figure 4a, the hot wire is heated to some resistance K times its resistance at ambient temperature (R_c) . The voltage across the heated element is

$$e_o = I_o KR_c \quad . \tag{2}$$

At some time t, a step input of heat or cooling is applied to the element. Sometime later with the input still applied, the system is in a steady condition and a new value of voltage measured across it is

$$e_o = I_o (KR_c - R_H) \tag{3}$$

where R_H is the resistance change caused by the applied input. From time t, to the time when steady state can be assured, the output voltage decreases exponentially. The model considered consists of two series resistors, fixed, and having a nonlinear function.

In the model used at Colorado State University Meteorological Tower the voltage output as a function of time starting from time t is given by

$$e_o(t) = I\ KR_c - I_o\ r_H \left(1 - e^{-\frac{t}{\tau_o}}\right) \quad . \tag{4}$$

The hot wire is placed in a bridge circuit which is balanced when the wire is heated to KR_c. As air passes the heated element, it causes the element to cool. The cooled element has a lower resistance which causes an unbalance in the bridge, thus, an error in signal e_1 (Figure 4b). This error signal is in turn amplified by a D.C. amplifier with gain -A, and again by a voltage-controlled current source. In essence, the error signal causes a corresponding change in the heater current, such that the resistance of the hot wire is returned to its original value KR_c. This system is a constant temperature anemometer. The two resistors R_2 and R_3 function only to balance the bridge current (I_o) as it passes through the hot wire.

The temperature sensors gave the absolute temperature reading at 22 ft and -.95 in., and the temperature difference between the upper (205 ft) and the middle level.

Data Analyses

In order to give a detailed picture of the small scale structure of atmospheric motion, a detailed evaluation of spectra was performed. The hot-wire signal was recorded on magnetic tape at the speed of 1 7/8 inches per second. For analysis of the signal the magnetic tape was played back at 60 inches per second. This increase in tape speed increases the actual atmospheric frequency variations by a factor of 32. It also reduces an hour of recorded data to less than 2 minutes of play-back time. A wave analyzer with a band width of one cycle and the ability to read down to two cycles per second in frequency was employed. This technique produces information down to 0.062 cycles per second. To read further down in frequency, the original data record was played back at tape speed of 30 inches per second and re-recorded at 1 7/8 inches per second. The second recording was then played back at 60 inches per second. This frequency upgrading produced an increase in the actual atmospheric frequency variation by a factor of 512. Thus, it is possible to obtain the information down to 0.0039 cycles per second. An hour of atmospheric recording is in this way reduced to about 10 sec play-back. The wave analyzer produces an output voltage proportional to the amount of energy at a given frequency. This output voltage fluctuates rapidly as the turbulent signal varies. In order to obtain a usable reading the output voltage must be integrated over a period of the signal. Therefore, the output at the wave analyzer is fed into an operational amplifier circuit integrator, and from there to a digital voltmeter. The frequency at which the measurement was made was indicated on an electronic counter. The output of the wave analyzer is proportional to the mean square voltage

and the output recorded by the integrator digital voltmeter is also proportional to this mean square.

The original signal was also decomposed into nine different wave numbers. The intermittency was calculated for each wave number and a flatness factor determined from the intermittency. To decompose the original signal into different frequencies four SKL variable electronic filters (Figure 5) and a GRC filter were used. High and low pass were set at the desired frequency. Playing the magnetic tape back at 1 7/8 inches per second .2 Hz, .7 Hz, 2.5 Hz, 12.0 Hz, and 50.0 Hz frequencies were obtained. After speeding up the magnetic tape by a factor of 32 frequencies 0.006 Hz, 0.02 Hz, 0.07 Hz, 0.3 Hz and 0.7 Hz were obtained. The output from the filters were recorded on an eight channel chart recorder.

To obtain scales of turbulence the autocorrelation function of the signals were computed

$$R(\tau) = \frac{1}{T}\int_{o}^{T} u(t)u(t+\tau)dt \qquad (5)$$

where T is the total integration time and $u(t)$ is the output of a hot wire (Bendat and Piersol, 1966). The autocorrelation is estimated by

1. Delaying $u(t)$ by a lag time τ .
2. Multiplying $u(t)$ at any instant by the $u(t-\tau)$ that occurred τ seconds before.
3. Averaging the instantaneous products over the sampling time.

The above operations are accomplished by the use of a Princeton Applied Research Model #101 correlation function computer (Figure 6). The total delay time of the computer ranges from 100 milliseconds

to 10 seconds. One hundred points of the correlation function were computed and stored for readout.

Since the autocorrelation function is a Fourier transform of the power spectra density function it is also possible to determine scales of turbulence spectrum measurements. For a quick look at the turbulent scales, just as a comparison to the scales obtained by autocorrelation functions, a sound and vibration analyzer was used. The analyzer consists of a preamplifier, filter and an output amplifier. The preamplifier section contains the amplification and attenuation necessary to change the input signal to the level convenient for filtering. Band widths of the filter are either 1/3 octave or 1/10 octave. The signal from the filter is amplified and recorded. The analyzer is continuously tunable from 2.5 Hz to 25 KHz in four decade ranges. The analyzer does not give the integration of a signal. The output is plotted in DB's.

In using the hot-wire data one must recognize that the signal is a function of fluid velocity and fluid temperature (Sandborn, Hot-Wire Anemometer Measurements in Large Scale Boundary Layers, 1967)

$$e = \frac{\partial E}{\partial U} u + \frac{\partial E}{\partial \overline{T}} t' \quad . \tag{6}$$

Thus, the RMS of the signal is

$$\overline{e^2} \simeq \left(\frac{\partial E}{\partial \overline{U}}\right)^2 \overline{u^2} + 2\left(\frac{\partial E}{\partial \overline{U}}\right)\left(\frac{\partial E}{\partial \overline{T}}\right)\overline{ut'} + \left(\frac{\partial E}{\partial \overline{T}}\right)^2 \overline{t'^2} \tag{7}$$

The temperature term can be neglected compared to the velocity term provided that $\Delta\overline{T}_w$ is greater than 800° F. So, under conditions where $\overline{ut'} = 0$ it is possible to measure RMS of the longitudinal fluid

velocity in the presence of temperature fluctuations. In the boundary layer $\overline{ut'}$ is of the order of $\sqrt{\overline{u^2} \times \overline{t^2}}$. Thus, this term cannot be dismissed lightly and the equation becomes

$$\overline{e^2} \simeq \left(\frac{\partial E}{\partial U}\right)^2 \overline{u^2} + 2\left(\frac{\partial E}{\partial U}\right)\left(\frac{\partial E}{\partial \overline{T}}\right)\overline{ut'} \tag{8}$$

The temperature sensitivity, $(\partial E/\partial \overline{T})$ is roughly equal to 0.1 $(\partial E/\partial U)$ for $\Delta T_w = 800°$ F. Thus, if $\overline{ut'}$ is of the same order as $\overline{u^2}$ then an error of 20% is made by neglecting the velocity-temperature term. For the present study the relation

$$\overline{e^2} \simeq \left(\frac{\partial E}{\partial U}\right)^2 \overline{u^2} \tag{9}$$

has been employed.

SMALL SCALE STRUCTURE

Spectrum

A very important problem in describing turbulent motion is the distribution of energy of fluctuations among the motions of different length scales. When placed in a turbulent flow, the hot wire has a very sensitive and quick response and gives an irregular curve of velocity vs. time without any apparent evidence of periodic components. Using Fourier analyses any function can be resolved into a series of harmonic components of different wave lengths. The mean value $\overline{u^2}$ will be made up of contributions of all frequencies, but, depending on the character of the field, fluctuations of certain frequencies will make important contributions and will thus largely determine the value of $\overline{u^2}$ while the effect of fluctuations of other frequencies will be negligible. Taylor has defined a spectrum function $F(f)$ to measure the fraction of total energy which is associated with a particular frequency f, so that $\overline{u^2}\,F(f)df$ is the contribution to $\overline{u^2}$ from frequencies lying between f and $f + df$ (Sutton, 1953)

$$\overline{u^2} = \int_0^\infty \overline{u^2}\,F(f)df \quad \text{or} \quad \int_0^\infty F(f)df = 1 \tag{10}$$

The spectrum function $F(f)$ is thought of as the energy density at a given frequency. For turbulence that is convected along the local mean velocity U a wave number k may be defined as

$$k = \frac{2\pi f}{U} \tag{11}$$

and a spectral function $F'(k)$ may be written as

$$\int_0^\infty F'(k)dk = 1 \tag{12}$$

Thus, the following relation must exist between $F(f)$ and $F'(k)$

$$F'(k) = \frac{U}{2\pi} F(f) \quad . \tag{13}$$

Both $F'(k)$ and $F(f)$ are energy densities. The wave number representation removes the mean velocity variation and is useful in spectrum comparison (Sandborn, 1969).

The spectrum function given in Figure 7 is the energy density function defined as

$$\int_0^\infty F(k)dk \equiv \frac{1}{B\overline{u^2_{TOT}}} \int_0^\infty \overline{u^2} F(k)dk \tag{14}$$

where B is the analyzer band width, $\overline{u^2}$ is the energy at k, and $\overline{u^2_{TOT}}$ is the mean square of the total fluctuation. Figure 8 shows a linear plot of digital voltmeter output versus wave number. The area under the curve was measured by a planimeter and was used in obtaining the value of $F(k)$. This technique requires only that the band width of the analyzer does not change with frequency.

The major point of interest in the spectrum on Figure 7 is the amount of energy in the extreme low frequencies. Classic spectra by Van der Hoven (1957) and Oort and A. Taylor (1969) show a decrease energy density at low frequencies such as one cycle per hour (10^{-4} cps) (dashed line in Figure 7). In order to obtain this decrease in energy it is necessary to have larger period recordings.

There is now overwhelming evidence that Kolmogorov's relation for the inertial subrange fits well the spectra of horizontal velocity components in neutral and unstable air provided that the height above

the ground is equal to or larger than the wave length considered (Panofsky, 1969). The relation is then

$$F(k) = b\,\varepsilon^{2/3}\,k^{-5/3} \tag{15}$$

where ε is the dissipation rate, k is the wave number and b is a constant. Indeed the spectrum in Figure 7 shows $F'(k) \alpha k^{-5/3}$ for the higher wave numbers.

Filtered Intermittency

The small scale structure of a random velocity field in a fully developed turbulent flow tends to be spatially localized. Since the viscous dissipation of turbulent kinetic energy occurs in the small scale structure, this implies that the region in which most of the dissipation occurs may be scattered through a fluid in a rather "spotty" way. As a measure of the intermittent nature of the small scale structure of turbulence, γ is defined as a fraction of time the detection probe sees the variable at a high amplitude state (Townsend, 1948). An indirect visualization of the intermittency of the small scale structure may be achieved by electronically examining narrow-band frequency components of the overall turbulent signal. Figures 9, 10, 11 and 12 show the original hot-wire anemometer signal and the same signal decomposed at nine different frequencies. It appears that all the signals are intermittent in time. By Taylor's hypothesis, frequency is proportional to wave number so the high frequency signals correspond to the velocity fluctuations associated with the small scale component of the motion. Also the temporal variation of a signal from a fixed hot wire corresponds to the space variation of the turbulent pattern. Therefore the intermittency of a

high frequency signal in the time domain implies the localization of the small scale structure in the space domain. The time interval when energy of high frequency is zero corresponds to the time when the hot wire is in the spatial region in which the small scale component is negligible. Figure 13 shows a plot of the intermittency factor γ versus wave number for different levels. The curves have only a slight increase at high wave numbers, and the value of γ does not change much with height with the exception, perhaps, of the 65 foot level at high wave numbers. The noise spectrum of the hot wire is constant with frequency, while the energy spectrum of turbulence decreases sharply with increasing frequency. Thus, the signal to noise ratio is small for high frequencies. In order to calculate the intermittency factor γ from the signal at different wave numbers, it was necessary to eliminate instrument noise. Figure 14 gives the intermittency factor γ plotted against signal amplitude ℓ shown on chart, Figure 9, for wave number 6.2. The curve drops off very rapidly from $\ell = 0$ to $\ell = 3$ mm when it becomes almost constant. So, for the signal of $k = 6.2$ the instrument noise has an amplitude of 3 mm. Similar plots of γ versus ℓ were plotted for each k in order to eliminate instrument noise. Intermittency of the small scale structure implies that the energy dissipation will appear intermittent, since the viscous dissipation of turbulent kinetic energy occurs primarily in the small scale structure.

An inherent characteristic of the SKL and GRC filters is their "ringing". It takes 3 cps for the SKL filter to damp out and 12-13 cps for a GRC filter. The amplitude-to-frequency response plotted around the set frequency f_o, gives, for the SKL filter, a wide peak and

straight sides on the curve, while the GRC filter has a very narrow peak and the sides have an inflection point. That is why a GRC filter "rings" more than a SKL filter. A GRC filter was used for high frequencies only.

Another measure of intermittency is the flatness factor or kurtosis

$$F.F. \equiv \frac{\overline{e^4}}{(\overline{e^2})^2} = \frac{\int_{-\infty}^{\infty} e^4 \, P(e)de}{\left[\int_{-\infty}^{\infty} e^2 \, P(e)de\right]^2} \qquad (16)$$

where e is a random variable and $P(e)$ is a probability density function. An intermittent signal of large amplitude will affect the "tails" and the center of the probability curve greatly. A random variable with normal density has a flatness factor equal to 3.0 and (F.F. - 3.0) for an arbitrary random variable is termed "coefficient of excess". The flatness factor can be used to indicate a degree of intermittency of a random variable only if it is known from other observations that the variable is intermittent, since a large flatness factor does not necessarily imply intermittency. Townsend (1948) suggested that the intermittency of a signal should be related to the flatness factor by

$$\gamma = \frac{3.0}{F.F.} \quad (x\ 100) \quad . \qquad (17)$$

Equation (16) leads to values greater than one for non-random signals. Thus, if $\gamma > 1$ there is a tendency toward periodic motion. Figure 15 shows the flatness factor plotted versus Reynolds number for the first derivative of velocity as computed by different authors. The present

investigation gives the flatness factor calculated from Figure 13 using Equation 16 for the velocity signal u at high frequencies.* Figure 15 shows reasonably good agreement of the present data with previous computations. The present data fall somewhat below the solid curve. These lower values may be due to filter ring errors.

The intermittency of the small scale structure implies that the energy dissipation, ϵ, is intermittent. It is possible to assume that only these intermittent regions where the turbulence occurs, contributes to the -5/3 variation of the spectrum the intermittency coefficient γ enters the constant b. It is evident then that the computation of ϵ is of particular interest. The general expression for ϵ is (Taylor, 1935)

$$\epsilon = \nu \left[2\overline{\left(\frac{\partial u}{\partial x}\right)^2} + 2\overline{\left(\frac{\partial v}{\partial y}\right)^2} + 2\overline{\left(\frac{\partial w}{\partial z}\right)^2} + \overline{\left(\frac{\partial v}{\partial x} + \frac{\partial u}{\partial y}\right)^2} + \overline{\left(\frac{\partial w}{\partial y} + \frac{\partial v}{\partial z}\right)^2} + \overline{\left(\frac{\partial u}{\partial z} + \frac{\partial w}{\partial x}\right)^2} \right] \tag{18}$$

where ν is the kinematic viscosity of the fluid. The restriction to isotropic turbulence leads to the simple form

$$\epsilon = 15\nu \overline{\left(\frac{\partial u}{\partial x}\right)^2} \quad . \tag{19}$$

---

*It is possible to compare present data with the flatness factor of $\partial u/\partial t$. Suppose that the signal is

$$u = A \sin ft$$

then

$$\frac{\partial u}{\partial t} = Af \cos ft$$

Thus the derivative of a signal is multiplied by frequency which does not change the F.F. very much, except for very high frequencies.

Sandborn and Braum (1956) have experimentally measured, in a wind tunnel, the rate of dissipation of turbulent kinetic energy (ε) given by isotropic relation (20) as a function of distance from the wall. In the same paper they present the calculation of ε from Klebanoff's data (1954). He obtained ε using Equations (18) and (19). The conclusion was that local isotropy was not found and the possible reason was the low value of Reynolds number.

The rate of turbulent energy per unit mass in isotropic turbulence is given by

$$\varepsilon = 2\nu \int_0^\infty k^2 E(k)dk \tag{20}$$

where k is the wave number and $E(k)$ is the three-dimensional spectrum function. Using the theory of isotropic turbulence the three-dimensional spectrum function can be related to the measurable one-dimensional spectrum function $F'(k)$ by

$$E(k) = \frac{1}{2} k^2 \frac{\partial^2 F'(k)}{\partial k^2} - \frac{1}{2} k \frac{\partial F'(k)}{\partial k} \quad , \tag{21}$$

(Hinze, 1959). In terms of the longitudinal one-dimensional spectrum, $F'(k)$ the expression for ε becomes

$$\varepsilon = 15\nu \int_0^\infty k^2 F'(k)dk \quad . \tag{22}$$

Using Taylor's definition of microscale

$$\frac{\overline{u^2}}{\lambda^2} = \int_0^\infty k^2 F'(k)dk \tag{23}$$

or

$$\lambda^2 = \frac{\overline{u^2}}{\overline{\left(\frac{\partial u}{\partial x}\right)^2}} \quad . \tag{24}$$

Equation (20) then becomes

$$\varepsilon = 15\nu \frac{\overline{u^2}}{\lambda^2} \tag{25}$$

and

$$\varepsilon = 15\nu \int_0^\infty k^2 F'(k)dk \quad . \tag{26}$$

Table 1 shows the calculation of ε for different levels. The value of the kinematic viscosity, ν, is 2×10^{-4} ft^2/sec. In order to obtain the value of the microscale of turbulence, λ, the data from Figure 7 were plotted on Figure 16. The integral under the curve gives the microscale of turbulence. In order to extrapolate the curve to the high frequencies, wind tunnel data were used.

TABLE 1

CALCULATION OF THE RATE OF DISSIPATION

Height (ft)	$U(\frac{m}{sec})$	$\frac{\varepsilon}{u^2}$	$\frac{\sqrt{\overline{u^2}}}{U_{loc}}$	λ(m)	$\overline{u^2}$	$\varepsilon(\frac{m^2}{sec^3})$
20	8.7	.256	.081	.0354	.495	.127
65	8.0	.274	.067	.0342	.286	.077
110	11.0	.148	.075	.0466	.692	.103
155	11.9	.118	.051	.0522	.368	.043

Table 2 shows the calculation of the constant b in Equation (14). The assumption was that the constant $b = A\gamma$, where A is a constant. Thus, the variation in γ would compensate for the variation in b and produce A as a constant value. The results in Table 2 show that γ does not vary very much, neither with height nor with wave number. The

rate of dissipation, ϵ , varies with height in a random way. As a result constant the A varies very much for the different levels. Thus, one can conclude that the intermittency factor γ enters the rate of dissipation, ϵ , and not the constant b . The average value for b is 0.7 which agrees very well with the value obtained by Russian authors (Lumley and Panofsky, 1964).

TABLE 2

CALCULATION OF CONSTANT b IN THE SPECTRA

h	k	ϵ	γ	F'(k)	$A\gamma = b$	A
20'	3.0	.127	.38	.021	0.28	.73
	10.0		.40	.0031	0.27	.66
	50.0		.42	.00022	0.027	.65
65'	3.0	.077	.55	.021	0.075	1.36
	10.0		.59	.0031	0.78	1.32
	50.0		.65	.00022	0.78	1.2
	100.0		.68	.00007	0.78	1.1
110'	3.0	.103	.26	.021	0.6	2.3
	10.0		.28	.0031	0.65	2.32
	50.0		.30	.00022	0.65	2.16
	100.0		.31	.00007	0.67	2.16
155'	3.0	.043	.36	.021	1.04	2.80
	10.0		.38	.0031	1.12	2.9
	50.0		.40	.00022	1.2	3.0
	100.0		.42	.00007	1.2	2.75

STABILITY EFFECTS

Richardson Number

Considering the balance between turbulence generating forces caused by shearing stress and alleviating forces produced by a stable stratification of the atmosphere, Richardson (1920) has developed a turbulence criterion. If the Richardson number, the ratio of these two forces, is smaller than a certain critical value, laminar flow will break into turbulence.

$$R_i = \frac{K_H}{K_M} \frac{\frac{g}{\bar{T}} \left(\frac{\partial T}{\partial z} + \Gamma \right)}{\left(\frac{\partial \bar{u}}{\partial z} \right)^2} \tag{27}$$

where K_H is the eddy diffusivity of heat, K_M is the eddy viscosity, g the acceleration of gravity, $\bar{T}$ the mean temperature, $\partial T/\partial z$ the observed vertical temperature lapse rate, Γ the dry adiabatic lapse rate, and $\partial \bar{u}/\partial z$ the vertical wind shear. Thus, the critical Richardson number determines the state of "just no turbulence", the condition between laminar and turbulent flow (Bunt, 1952; Sutton, 1953; Hess, 1959). In his original work Richardson assumed $K_H/K_M = 1$. He asserted that if the motion is slightly turbulent it will remain turbulent if $R_i < 1$ and will subside into a laminar flow if $R_i > 1$. The value of $K_H/K_M = 1$ has been found in laboratory measurements (Lumley and Panofsky, 1964). In the free atmosphere this value depends on stability and values as large as 3 have been found in unstable air. The viscous dissipation of kinetic energy has been neglected in the original derivation (Calder, 1949). This could reduce the critical Ri number but its effect is hard to evaluate.

As can be seen from Equation (27), in order to calculate the value of the Richardson number it is necessary to know only the vertical wind profile and the temperature lapse rate. Figures 7, 8 and 9 show the mean wind velocity taken during the 24 hour period on May 9 and 10, 1968 at three different levels. Figure 20 is a plot of temperature lapse rate between 200 and 20 feet over the same period of time. Wind data had to be interpolated at the 20 ft level in order to obtain Ri. In the early afternoon hours the vertical wind shear is very low and the Richardson number has a very large value, $R >> 1$, which would indicate that turbulent conditions would not remain. In the early evening hours and during the night the wind was very strong and the wind shear quite large. The resulting Richardson number is very close to zero and certainly $Ri < 1$, which means that the flow was turbulent. About 7 a.m. on May 10 the Richardson number increased again to a value higher than 1.

Scales of Turbulence

A statistical description of turbulent motion includes a detailed look at the correlation between the velocities at two or more points in the flow and the "scales" of motion contributing to the signal. The correlation between two points in the flow in a turbulent field was suggested by Taylor (1935) as a means of looking at eddy sizes in a turbulent field. The turbulent velocities at two points will be correlated if they are related to the same eddy. The expectation is that the correlation will diminish as the distance between the points increase. If $R(x)$ is a space correlation coefficient between points separated by distance x, that is

$$R(x) = \frac{\overline{u_1 u_2}}{\sqrt{\overline{u_1^2}}\ \sqrt{\overline{u_2^2}}} \quad . \tag{28}$$

Taylor defines two lengths

$$L \equiv \int_0^\infty R(x)dx \tag{29}$$

and

$$\frac{1}{\lambda^2} \equiv \lim_{x \to o} \left(\frac{1-R(x)}{x^2} \right) \tag{30}$$

provided that $R(x)$ is zero for x greater than some finite length (meaning that the integral converges). The length L, called the integral or macroscale of turbulence, represents the average size of the eddies without implying any definite model of an eddy. The length λ is called the microscale of turbulence and is the measure of the average "diameter" of the smallest eddies, or the length scale of the fluctuations which are mainly responsible for the dissipation of energy. λ is the intercept at the x axis of the parabola drawn to touch the $(R(x), x)$ curve at its vertex. It is questionable whether or not turbulence in the boundary layer should be described in terms of eddies. Thus, the lengths L and λ are characteristic lengths associated with the scale of turbulent motion in a turbulent boundary layer, but the identification of eddies is not necessary in this definition of "scale".

According to Taylor's hypothesis (1938), if the mean wind speed is high enough the turbulence will not have time to change as it is convected past a point. The only requirement for homogeneous flow in a boundary layer is that the scales of motion are smaller than the height at which the measurement is taken. This hypothesis then allows the time

correlations and spectra to be interpreted in terms of the space variables. The transformation of coordinates used is $x = Ut$. The length scales L and λ can be calculated by using the time autocorrelation function

$$L = U \int_0^\infty R(t)dt \tag{31}$$

$$\frac{1}{\lambda^2} = \lim_{t \to o} \left(\frac{1-R(t)}{t^2} \right) \quad . \tag{32}$$

Figure 21 shows the autocorrelation function obtained by taking a product of two values of $u(t)$ at time t and $t + \tau$ and averaging over D = 45 min period, using the Princeton Correlator. Both autocorrelation curves on Figure 21 were obtained using the same signal $u(t)$; the only difference is in the time delays. The top one has $\tau = 6.4$ sec delay and the bottom one has $\tau = 32$ sec. L was calculated from the area under the curve. Figures 23, 24, 25, and 26 give the integral scales of turbulence over the 24 hour period. The hot-wire anemometers were rotated always to face into the wind and they were measuring the longitudinal component of wind. The scales obtained from all four of the anemometers are of the same order of magnitude. Figure 27 is the 24 hour variation of mean of the four length scales. This figure compared with Figure 21 shows that the length scale L had the smallest value for very large Reynolds numbers.

Taylor has shown in his original paper on "spectrum of turbulence" that the spectral function can be related to the correlation function $R(t)$

$$F'(k) = \frac{2}{\pi} \int_0^\infty R(t) \cos kt dt \tag{33}$$

or

$$R(t) = \int_0^\infty F'(k) \cos ktdt \quad . \tag{34}$$

Since the correlation function in time is a Fourier transform of the spectrum function in time. Using Taylor's hypothesis again, $x = Ut$

$$F(f) = \frac{4}{U} \int_0^\infty R(x) \cos \frac{2\pi f}{U} dx \quad . \tag{36}$$

The scale L is then given by

$$\frac{4L}{U} = \frac{4}{U} \int_0^\infty R(x)dx = F(o) \quad . \tag{37}$$

The integral scale defined by Equation (30) is related to the spectral function at zero frequency

$$L = \frac{U\, F(o)}{4} \tag{38}$$

the microscale is defined in terms of spectra as

$$\frac{1}{\lambda^2} = \frac{2\pi^2}{U} \int_0^\infty f^2 F(f)df \quad . \tag{39}$$

λ depends on f^2 which indicates that it depends mainly on high frequencies, or on small scale turbulence.

Figures 28 and 29 give the length scale L calculated from the spectra during the 24 hour period. The order of magnitude and the variation of L in time agrees very well with the results in Figures 24 and 25.

CONCLUSIONS

The purpose of the present investigation was to compute turbulence characteristics using highly accurate measurements of wind fluctuations obtained by hot-wire anemometers. All the characteristics were computed using analog computing techniques. Two separate runs were conducted with a different distribution of the hot-wire anemometers. During the first run four of the anemometers were distributed vertically along the tower. The spectrum and the filtered intermittency were studied using this data. The second run had four anemometers in a horizontal line at the top of the tower. Integral scales of turbulence were computed out of autocorrelation functions and spectra were calculated with these data.

The results show that the spectra follow the -5/3 law of Kolmogorov but the decrease in energy density for the low wave numbers ($k \leq 10^{-3}$ in.) did not show. In order to obtain this "gap" in the spectra it would be necessary to take observations over longer periods.

It is shown that the velocity signal is intermittent. The intermittency factor γ, was calculated for each of the nine frequencies into which the original signal was decomposed and plotted versus wave number. It is shown that γ does not vary much with the wave number or the height above the ground. As a measure of intermittency the flatness factor of the signal $u(t)$ was calculated and compared with the flatness factor of the first derivative of the signal computed by Batchelor and Townsend, Kuo, Wygnansky and Wyngaard. The present data fit the curve very well for high Reynolds numbers. The Richardson number was computed for a 24 hour period. As a measure of stability conditions during this period the scales of turbulence were obtained.

It is shown that the conditions were rather stable during the afternoon when the scales of turbulence have their minimum value. During the night the wind increased, the conditions became unstable and the scale of turbulence increased.

REFERENCES

REFERENCES

Baldwin, L. V. and Sandborn, V. A., 1967: Intermittency of Far Wake Turbulence, Colorado State University, CEP67-68LVB-VAS1, Fort Collins, Colorado.

Batchelor, G. K., 1953: The Theory of Homogeneous Turbulence, Cambridge University Press.

Bendat, J. S. and Piersol, A. G., 1966: Measurement and Analysis of Random Data, John Wiley & Sons Inc. New York, N. Y. p. 390.

Brunt, D., 1952: Physical and Dynamical Meteorology, Cambridge Univ. Press, p. 428.

Calder, K. L., 1949: The Criterion of Turbulence in a Fluid of Variable Density With Particular Reference to Conditions in The Atmosphere, Quarterly Journal of Royal Meteorological Society, pp. 71-78.

Corrsin, S. 1943: U.S. National Advisory Committee for Aerospace, War Report W94 , 1943.

Finn, C. L. and Sandborn, V. A., 1964: Instrument for Measuring the Intermittency of Quasi Steady Signals, Oct. 1964, Fluid Mechanic Papers, Colorado State Univ., Fort Collins, Colorado.

Finn, C. L. and Sandborn, V. A., 1967: The Design of A Constant Temperature Hot-Wire Anemometer, International Synmposium on Hot-Wire Anemometry, Univ. of Maryland, March 20-21, 1967.

Hess, S. 1959: Introduction to Theoretical Meteorology, Henry Holt & Co., New York, p. 362.

Hinze, J. O., 1959: Turbulence, McGraw Hill, New York.

Kolmogorov, A. N., 1941: The Local Structure of Turbulence in an Incompressible Viscous Fluid of Very Large Reynolds Number, C. R. Acad. of Sci. USSR, Vol. 30, p. 301.

Kolmogorov, A. N., 1962: A Refinement of Previous Hypothesis Concerning The Local Structure of Turbulence in a Viscous Incompressible Fluid At High Reynolds Number, Jour. of Fluid Mech. Vol. 13, p. 82.

Kuo, Albert Yi-shuong, 1970: Experiments on the Internal Intermittency in Turbulent Flow, Ph.D. Thesis, Dept. of Mech. John Hopkins, Univ. Baltimore, Maryland

Lin, C. C., 1948: Note on the Law of Decay of Isotropic Turbulence, Proc. of the National Acad. of Sci. Vol. 34, pp. 540-543.

Lumley, J. L. and Panofsky, H. A., 1964: The Structure of Atmospheric Turbulence, Monographs and Text in Physics and Astronomy, John Wiley and Sons, New York, N. Y.

Oboukhov, A. M., 1962: Some Specific Features of Atmospheric Turbulence, Jour. of Fluid Mech. Vol. 13, p. 77.

Reiter, E. R., 1967: Meteorological Conditions at the Fort St. Vrain Nuclear Generating Station, June 1967, Atmospheric Science Dept. Colorado State Univ., Fort Collins, Colorado.

Reiter, E. R. and Lester, P. F., 1967: The Dependence of the Richardson Number on Scale Length, Atmospheric Science Paper No. 3, Colorado State University, Fort Collins, Colorado.

Richardson, L. F., 1920: The Supply of Energy From and To Atmospheric Eddies, Proc. of the Royal Society, A97- pp. 354-373.

Sandborn, V. A. and Braum, W. H., 1956: Turbulent Shear Spectra and Local Isotropy in the Low-Speed Boundary Layer, NACA TN 3761, Lewis Flight Propulsion Laboratory, Cleveland, Ohio.

Sandborn, V. A., 1969: Boundary Layer Turbulence (Class Notes), College of Engineering, Colorado State Univ., Fort Collins, Colorado.

Sandborn, V. A., 1966: Metrology of Fluid Mechanics, College of Engineering, Colorado State Univ., Fort Collins, Colorado CER66-VAS32, p. 113.

Sandborn, V. A., 1967: Hot-Wire Anemometer Measurements in Large-Scale Boundary Layers, International Symposium On Hot-Wire Anemometry, Univ. of Maryland, March 20-21, 1967.

Sheih, C. M., 1969: Airborne Hot-Wire Measurements of the Small Scale Structure of Atmospheric Turbulence, Dec. 1969, Ph.D. Thesis, Penn. State, Dept. of Airspace Engr.

Stewart, R. W., 1969: Turbulence and Waves in a Stratified Atmosphere, Proc. of Colloquium on Spectra of Meteorological Variables, June 1969, Stockholm, Sweden.

Sutton, O. G., 1953: Micrometeorology, McGraw-Hill Book Co., 1953, p. 96.

Taylor, G. I., 1921: Diffusion by Continuous Movements, Proc. of the London Mathematical Society, Series 2, 20., pp. 196-211.

Taylor, G. I., 1935: Statistical Theory of Turbulence, Parts I-IV. Proc. of the Royal Society, A151- pp. 421-278.

Taylor, G. I., 1938: The Spectrum of Turbulence, Proc. of the Royal Society, A164, pp.476-490.

Tieleman, H. W., 1967: Viscous Region of Turbulent Boundary Layer, Ph.D., Thesis, Colorado State Univ. College of Engineering, Fort Collins, Colorado.

Townsend, A. A., 1948: Local Isotropy in the Turbulent Wake of a Cylinder, Australian Jour. Sci. Res., Series A., Vol. I, p. 161.

Vinnichenko, N. K. and J. A. Dutton, 1969: Empirical Studies of Atmospheric Structure and Spectra in the Free Atmosphere, Proc. on Colloquium on Spectra of Meteorological Variables, Stockholm, Sweden, June 9-19, 1969.

FIGURES

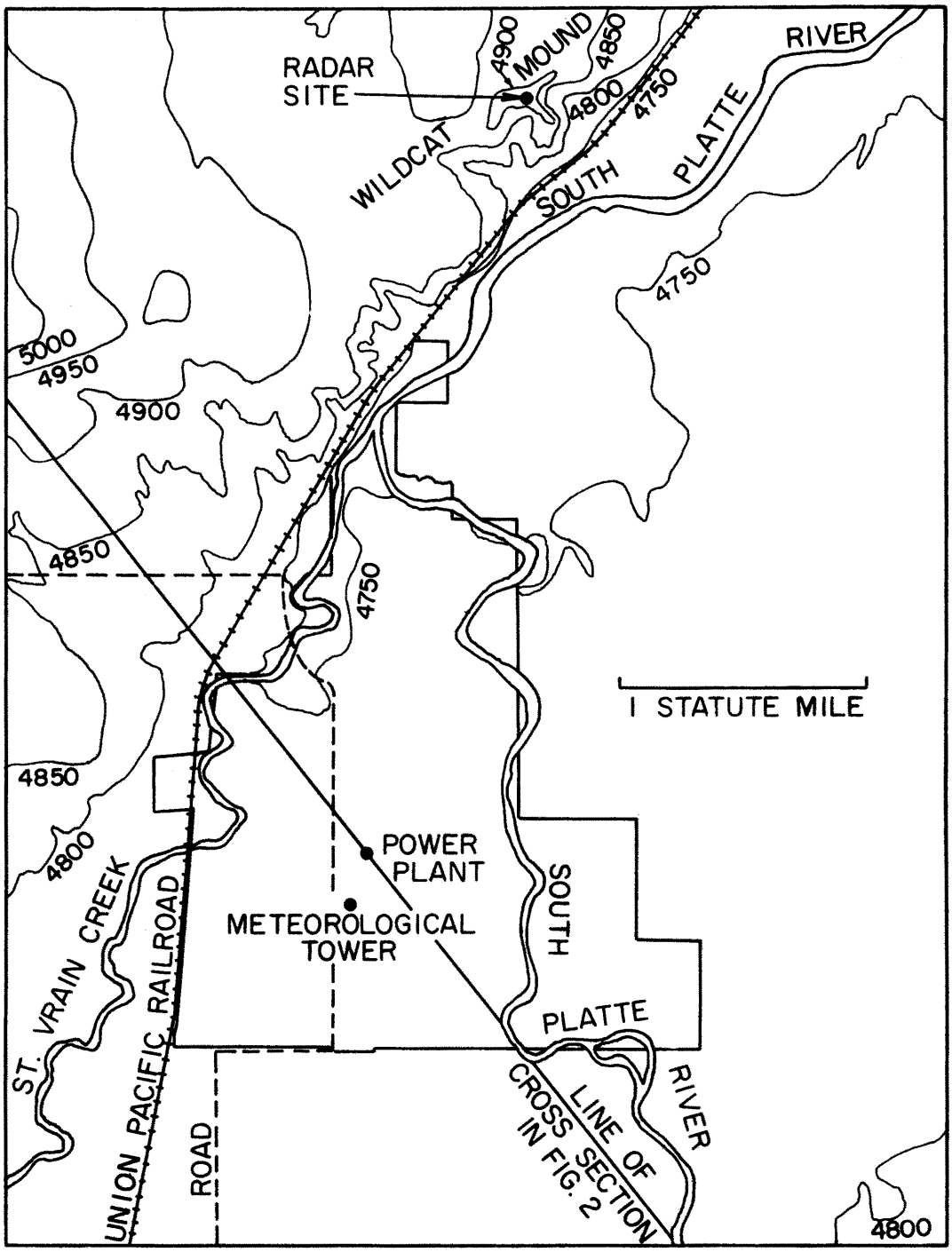

Fig. 1 Detailed map of the meteorological tower. Height contours are given in feet. The straight line indicates the plane of the cross section in Fig. 2. (Reiter, 1967, Meteorological Conditions at the Fort St. Vrain Nuclear Generating Station).

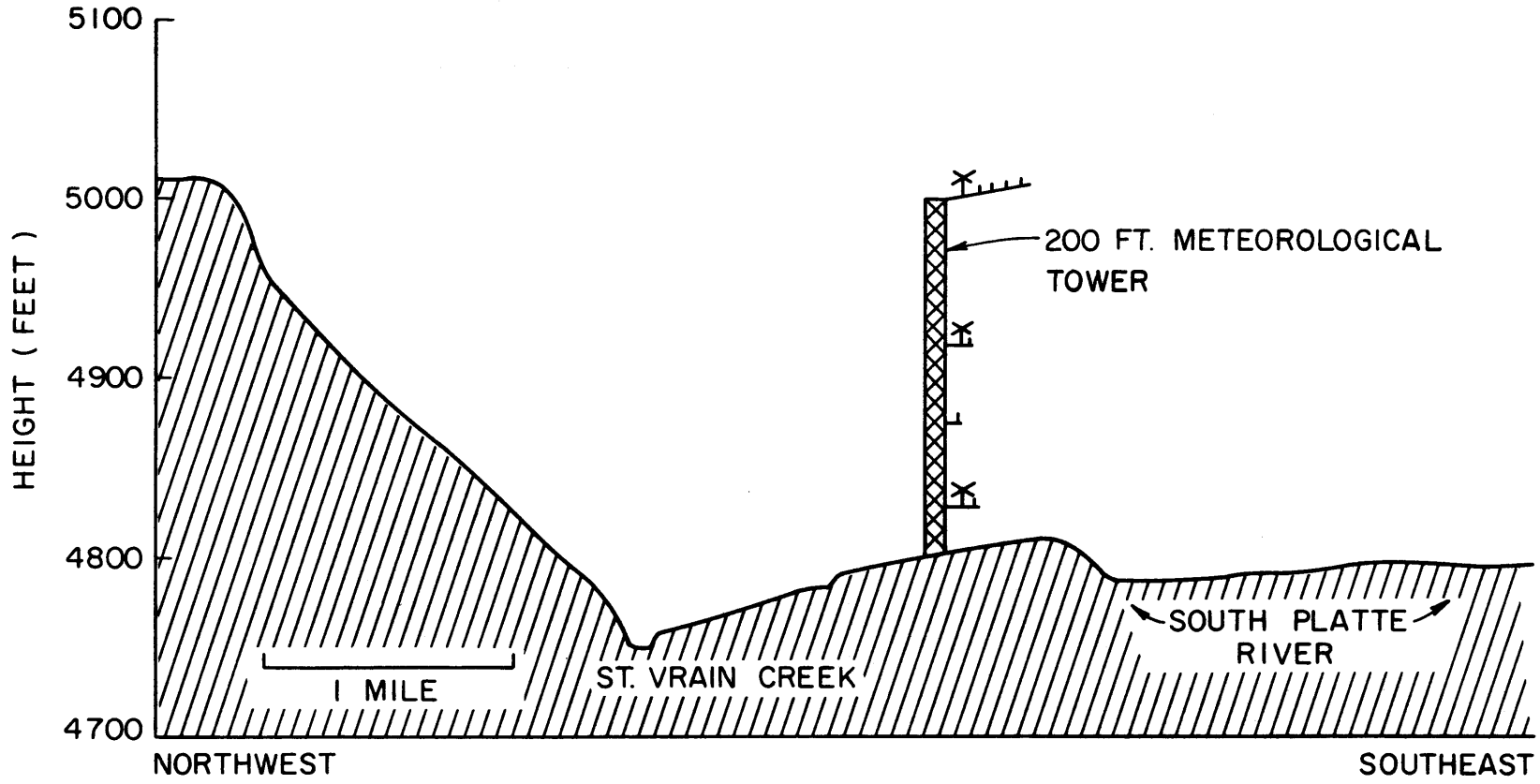

Fig. 2 Terrain cross section as indicated in Fig. 1, with meteorological tower and the position of hot wire and cup anemometer. (Reiter, 1967, Meteorological Conditions at the Fort St. Vrain Nuclear Generating Station.)

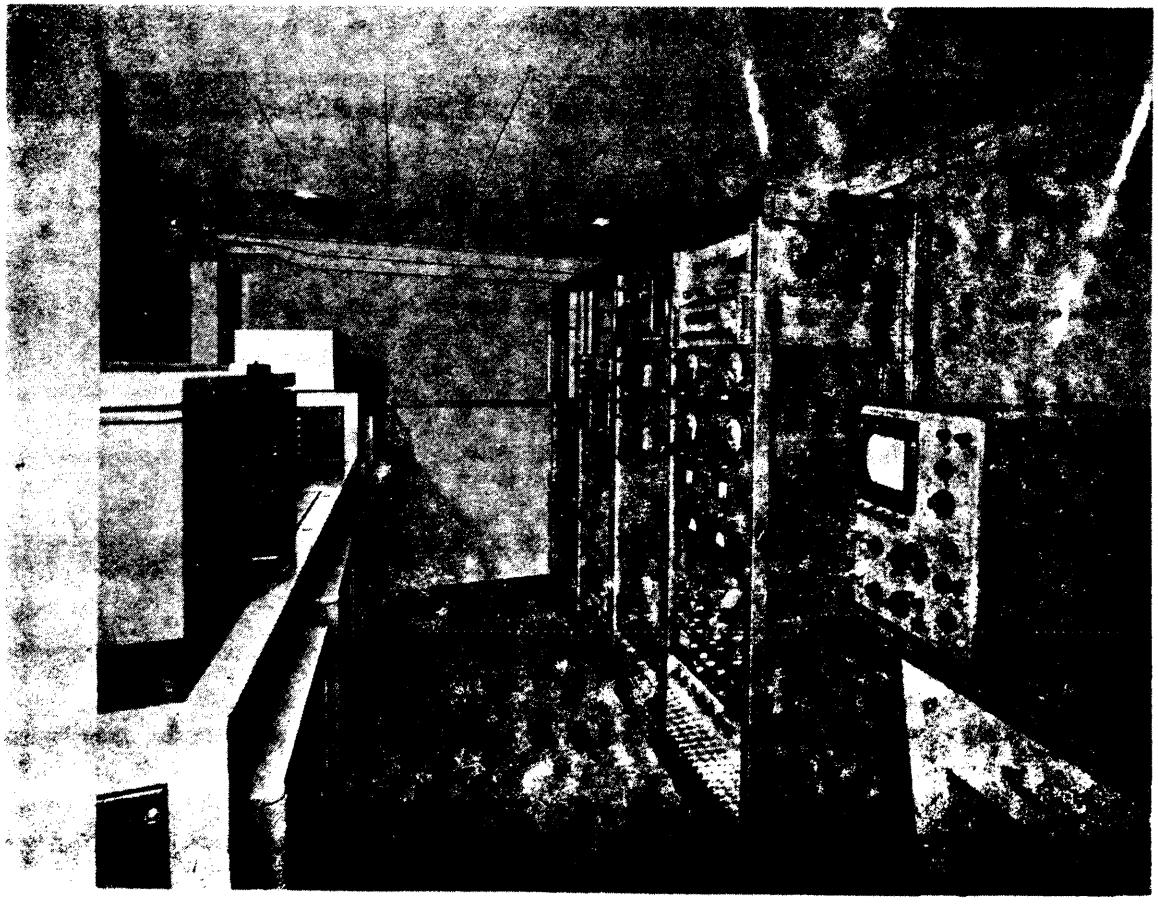

Figure 3. Inside of instrumentation and analog computation van.

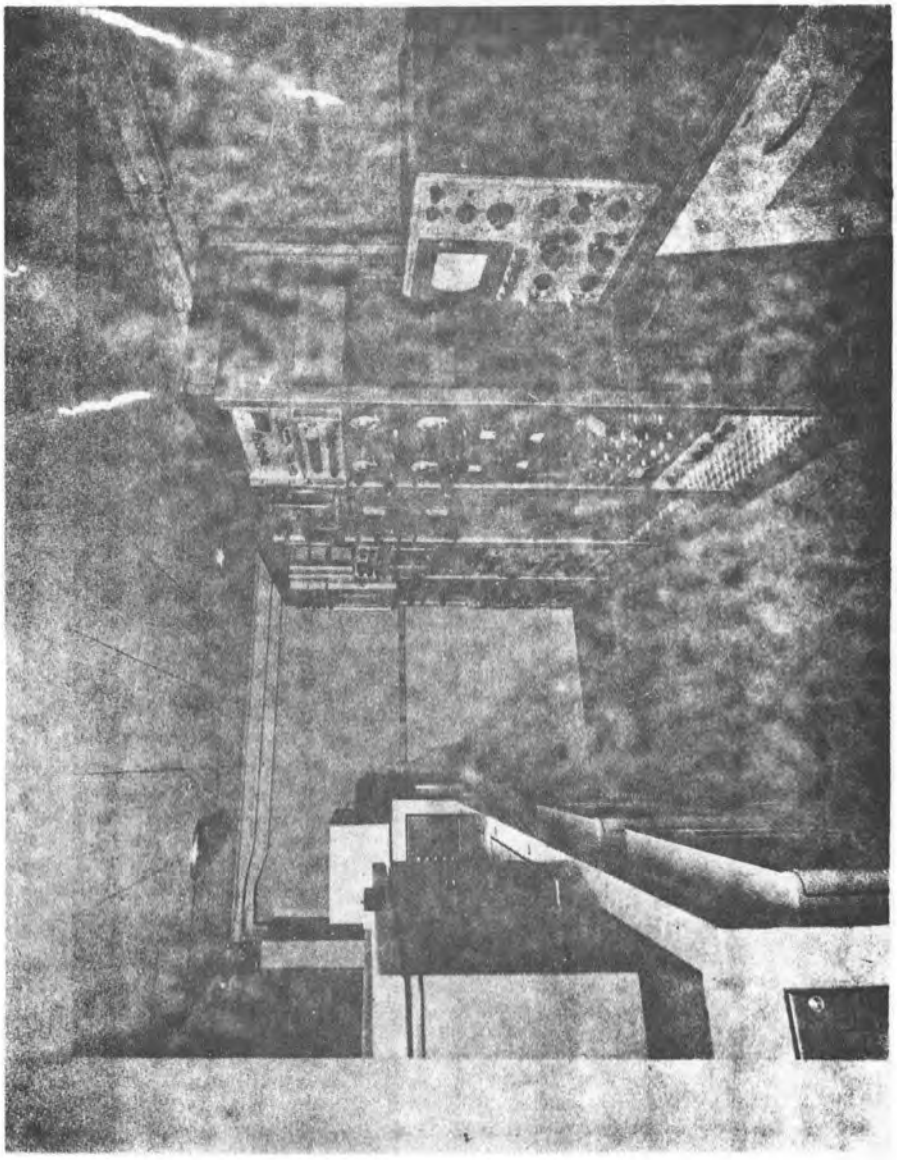

Figure 3. Inside of instrumentation and analog computation van.

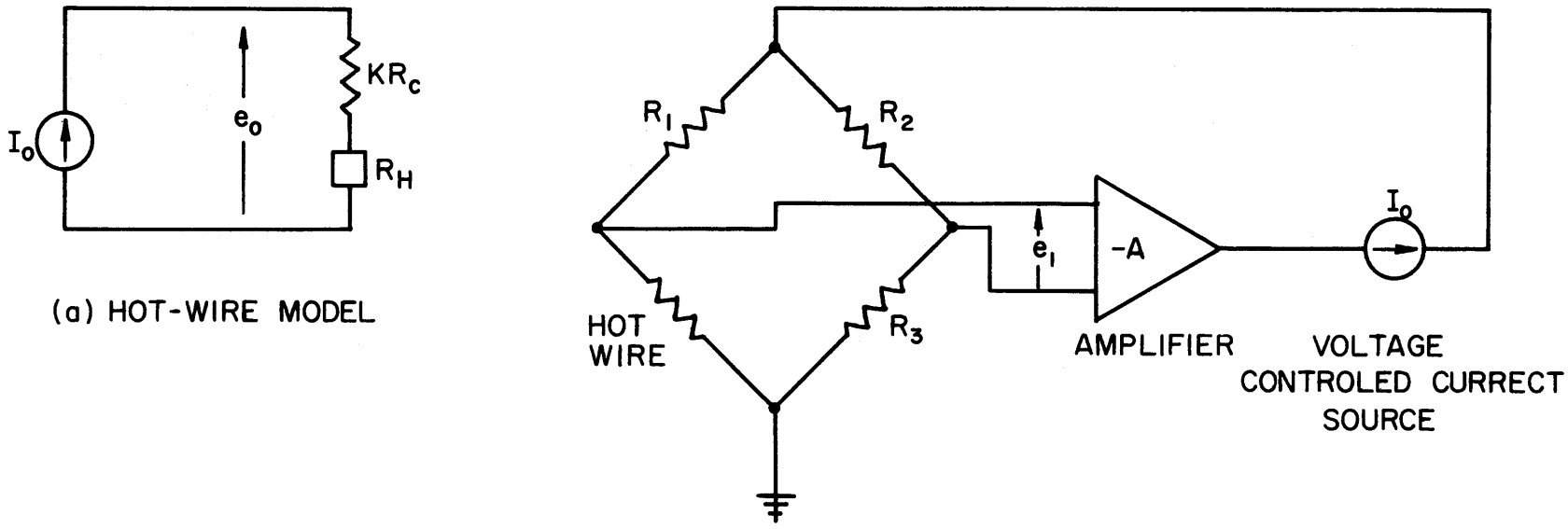

Fig. 4 Schematic diagram of hot-wire anemometry used at the CSU meteorological tower (C. L. Finn and V. A. Sandborn: The design of a constant temperature hot-wire anemometer, 1967).

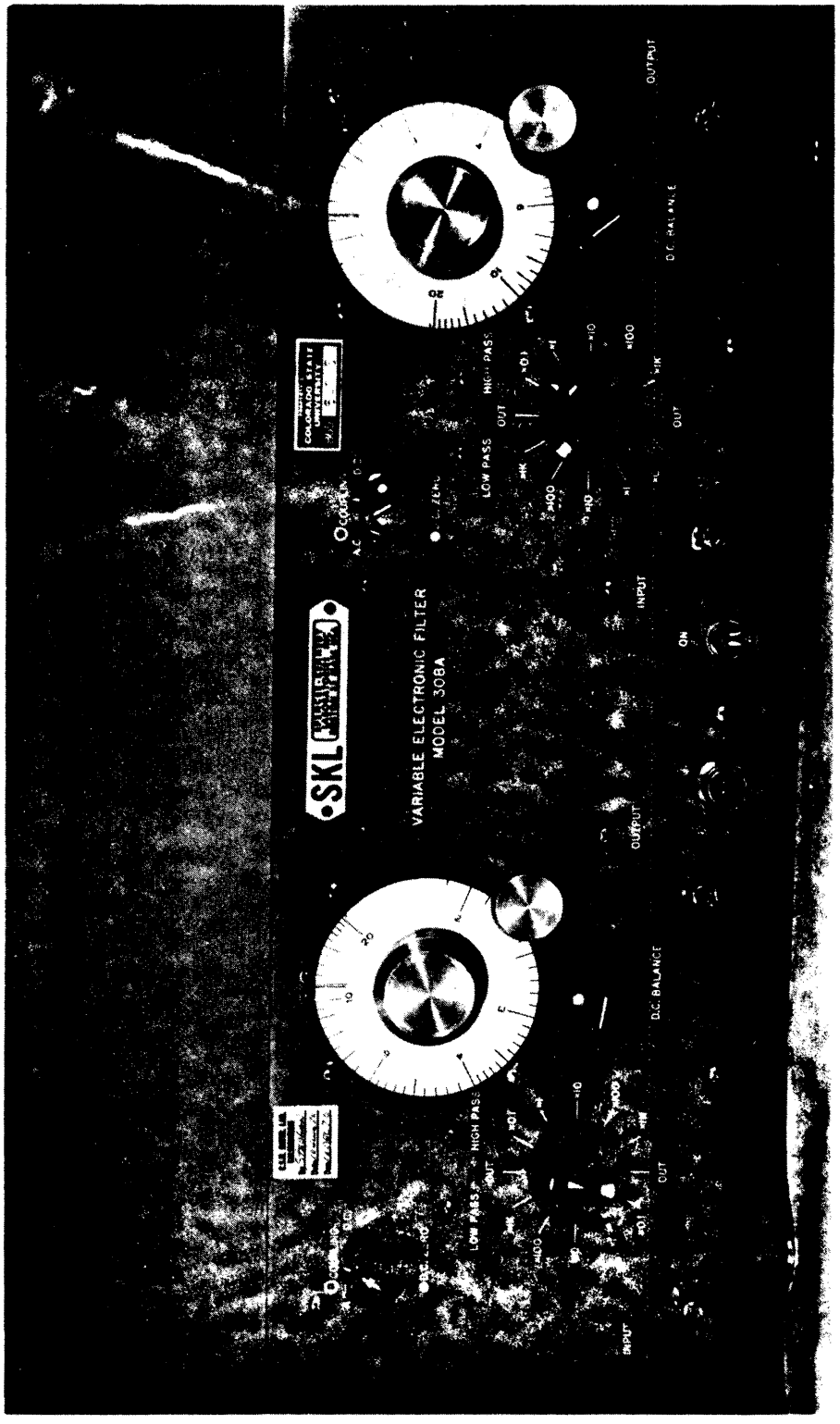

Figure 5. Variable electronic filter.

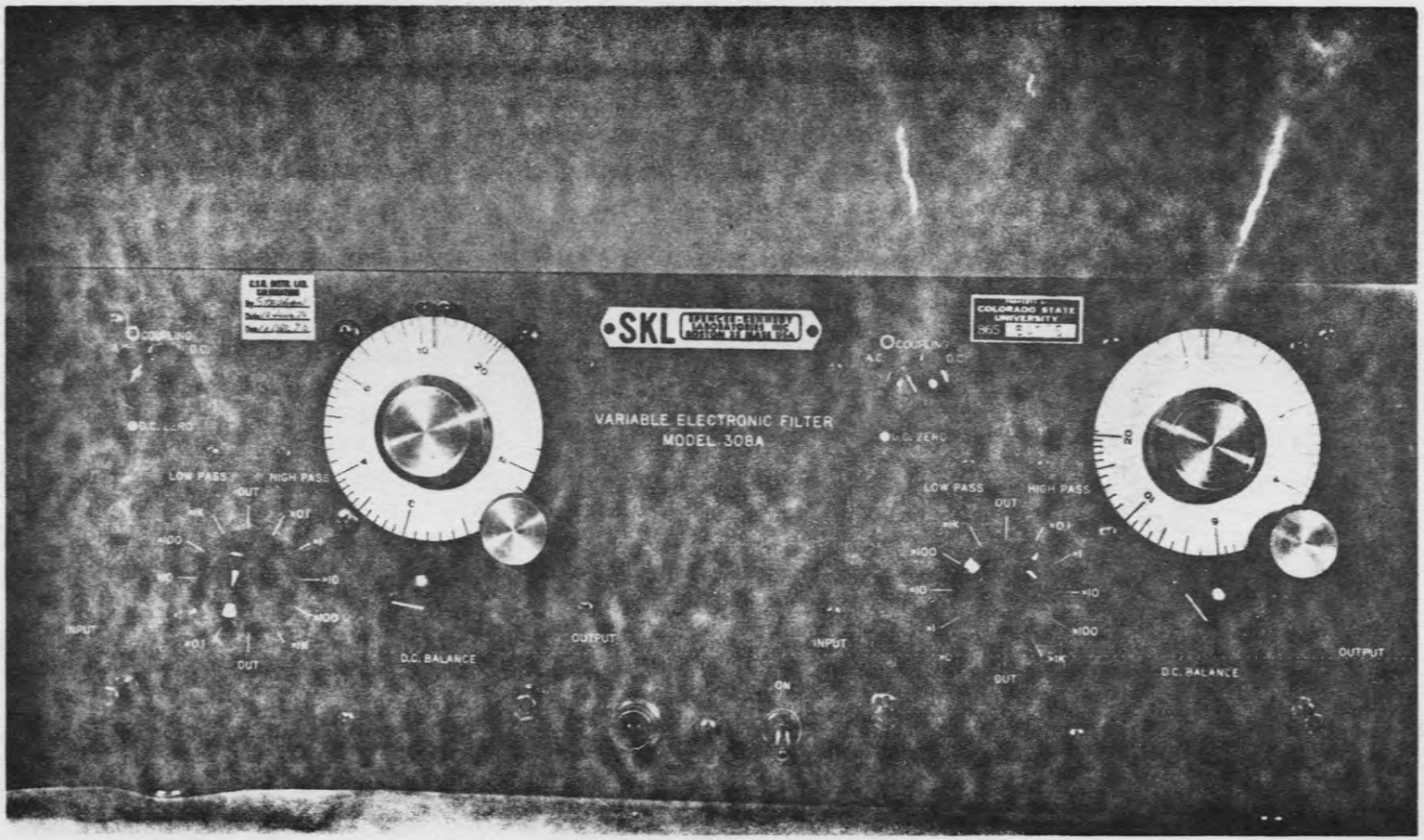

Figure 5. Variable electronic filter.

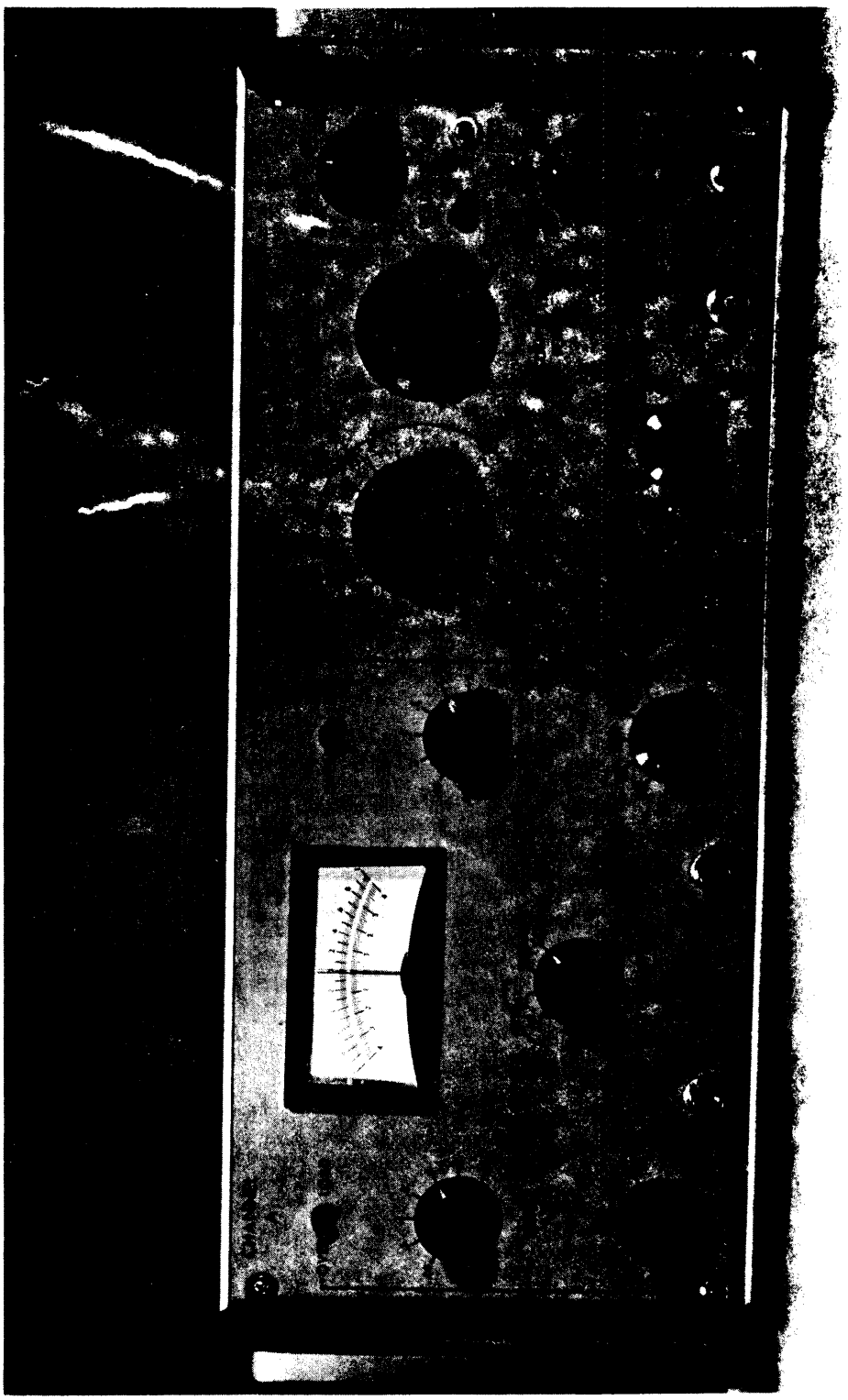

Figure 6. PAR Model 101 signal correlator.

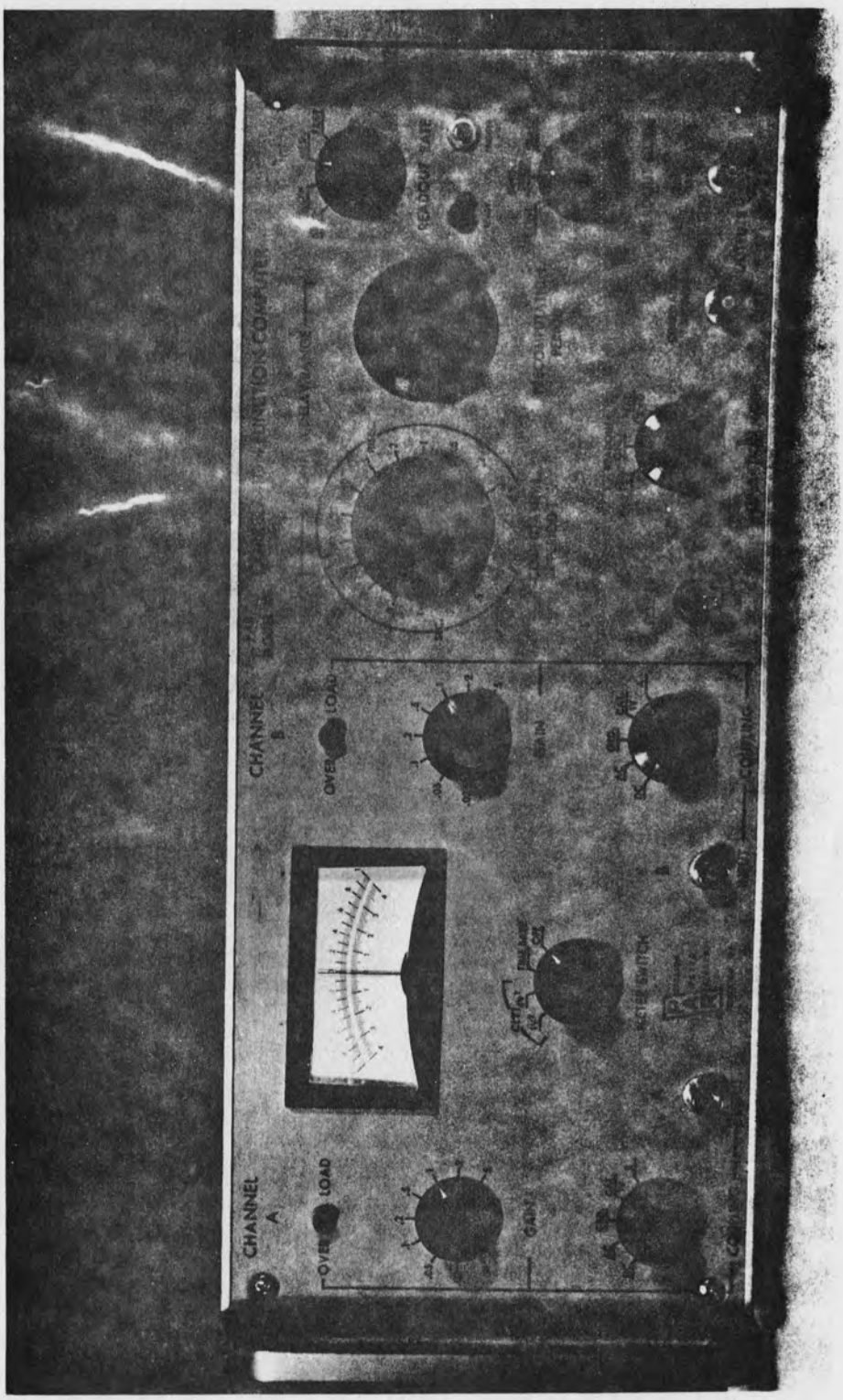

Figure 6. PAR Model 101 signal correlator.

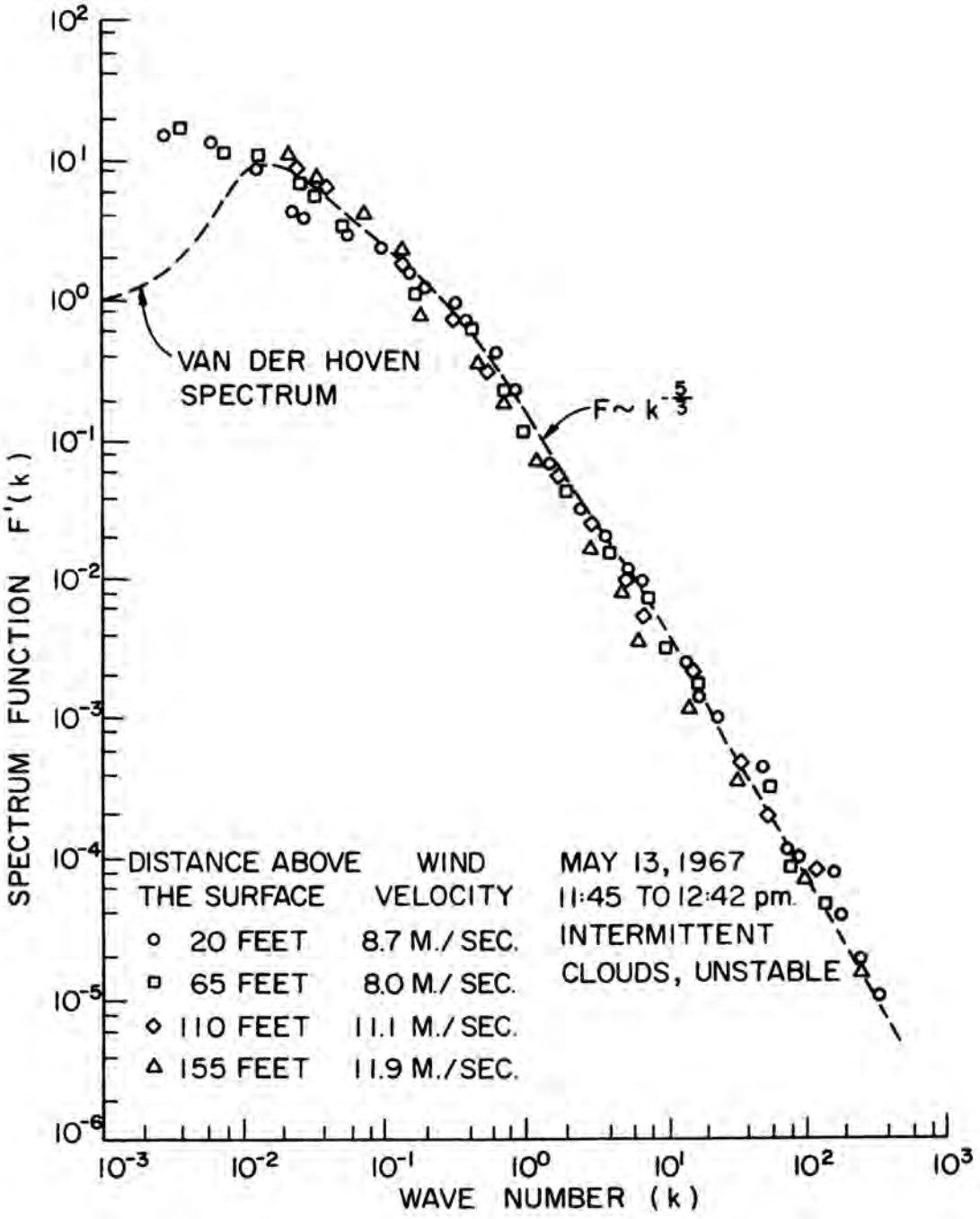

Fig. 7 Spectrum of atmospheric turbulent energy at high frequencies.

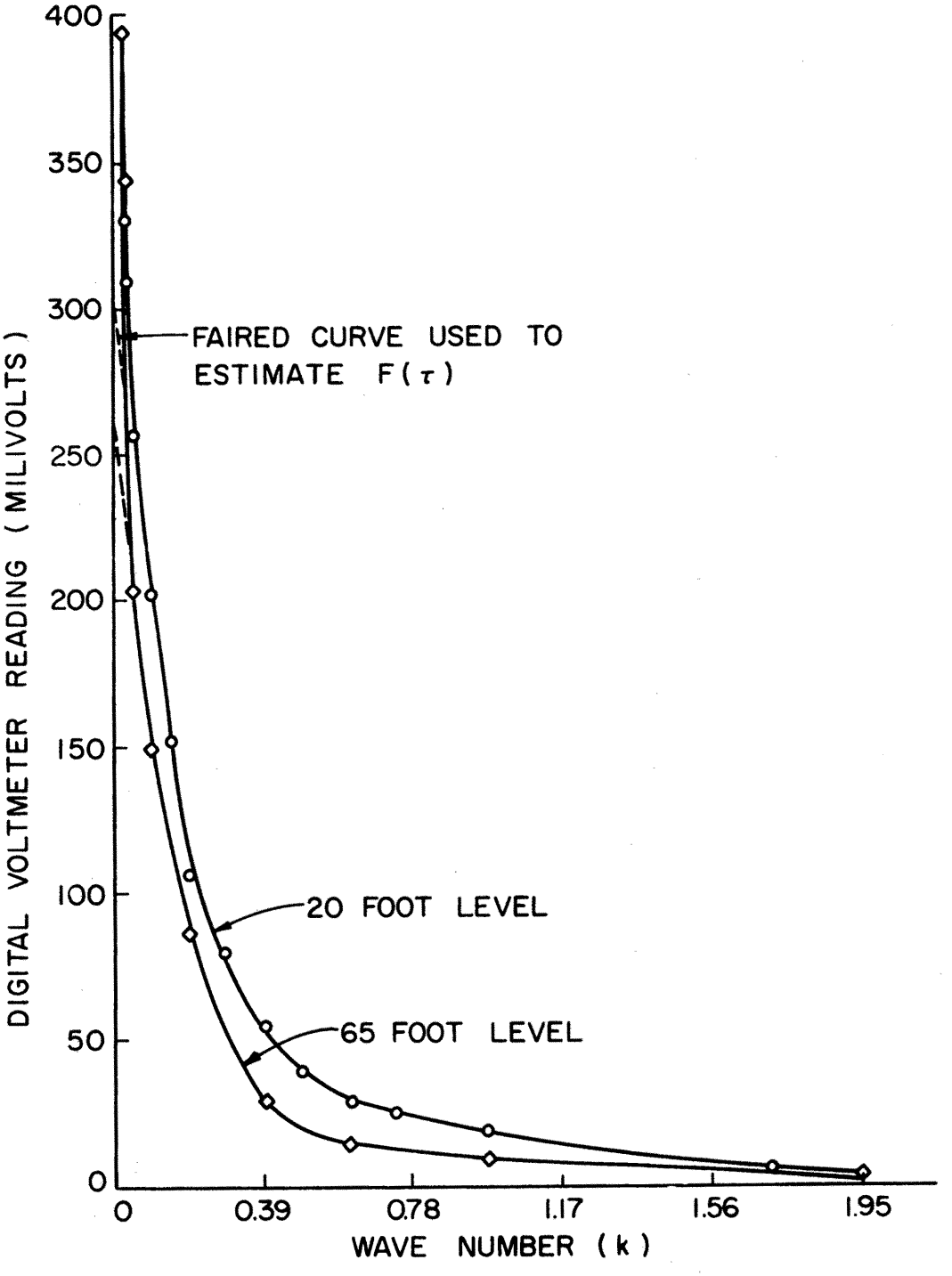

Fig. 8 Cruves used to compute F'(k).

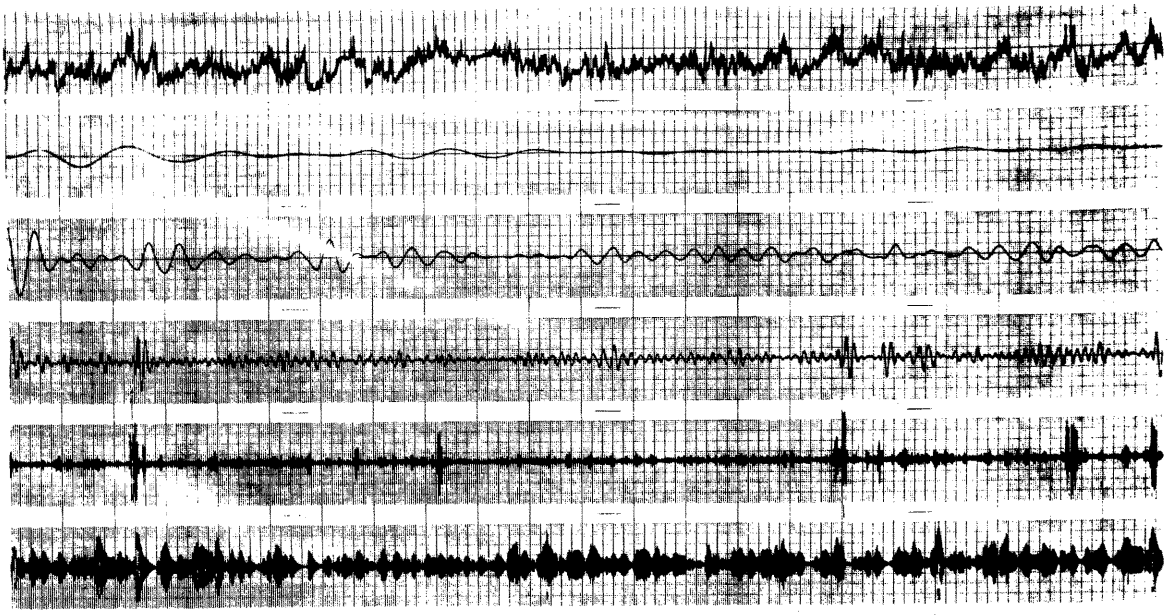

Chart speed 1 cm/sec

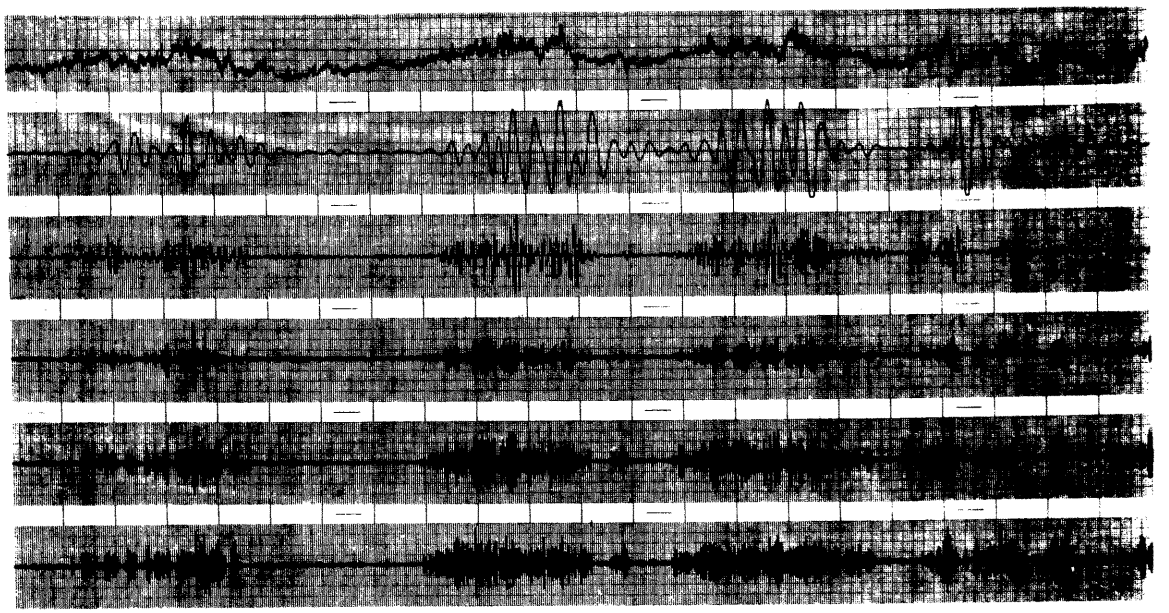

Chart speed .2 cm/sec

Fig. 9 20 foot level signal and the same signal decomposed on the different frequencies

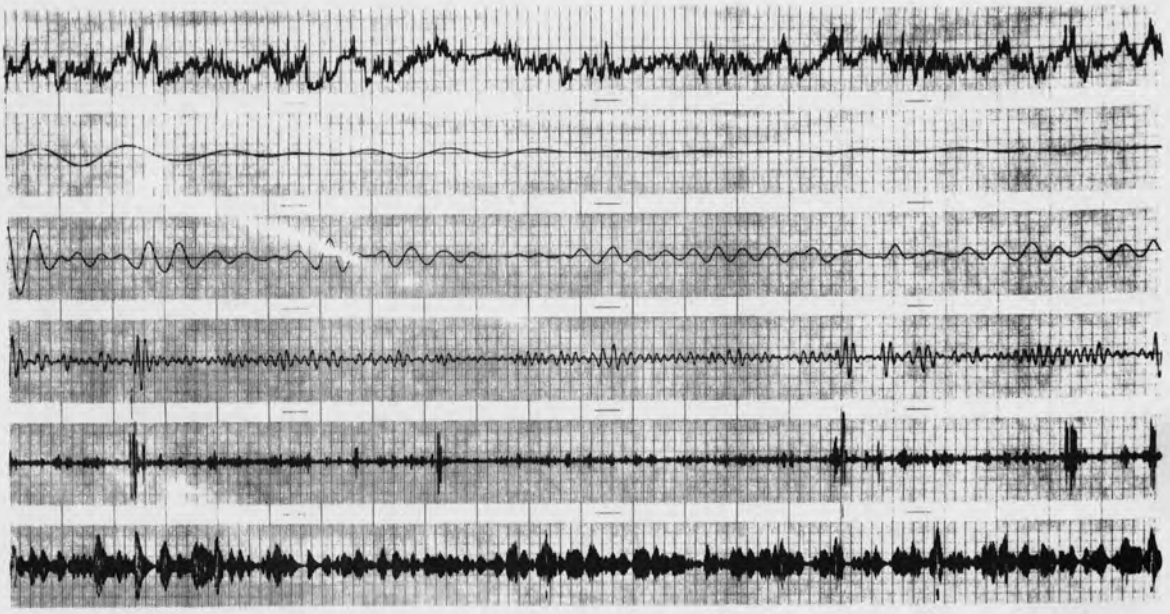

Chart speed 1 cm/sec

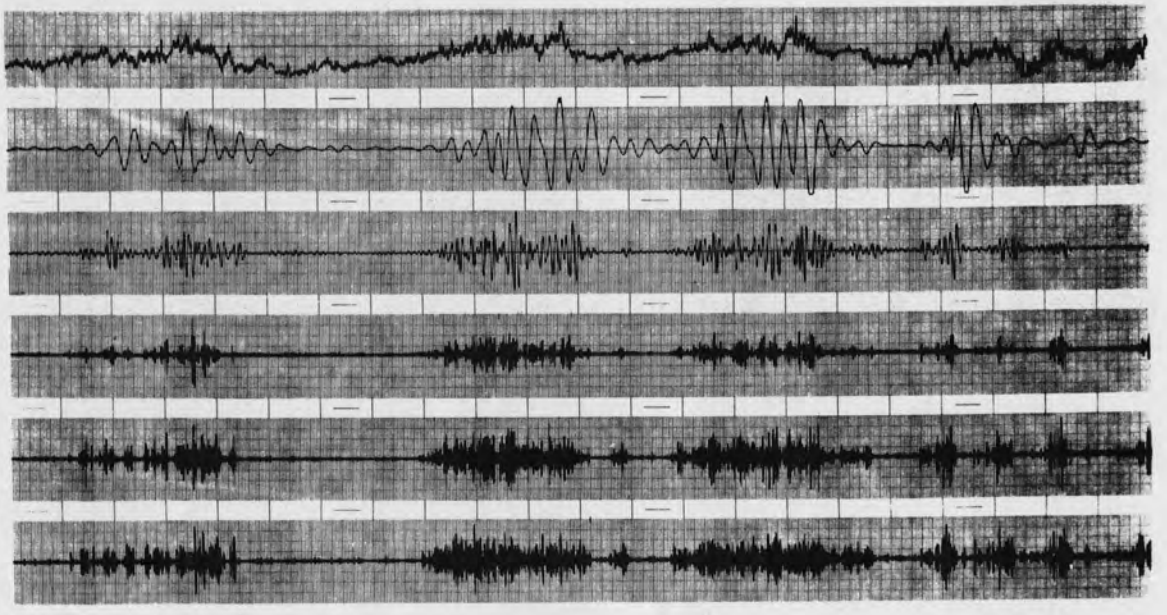

Chart speed .2 cm/sec

Fig. 9 20 foot level signal and the same signal decomposed on the different frequencies

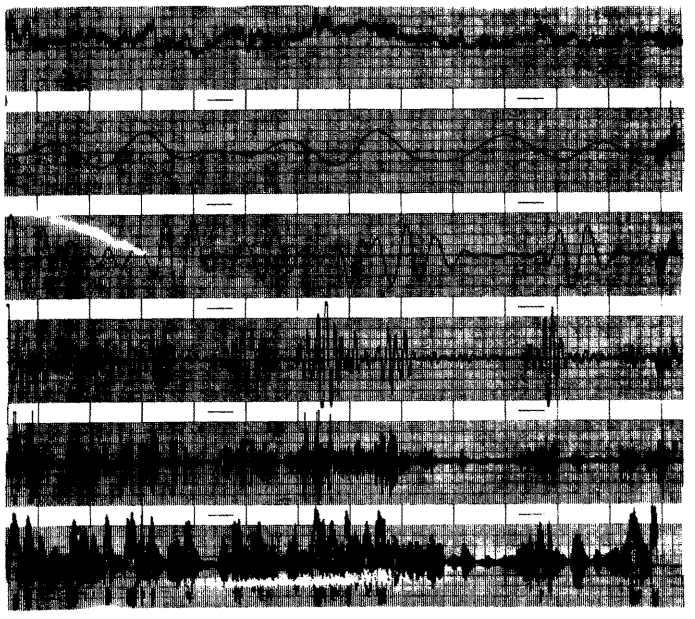

Chart Speed 1 cm/sec

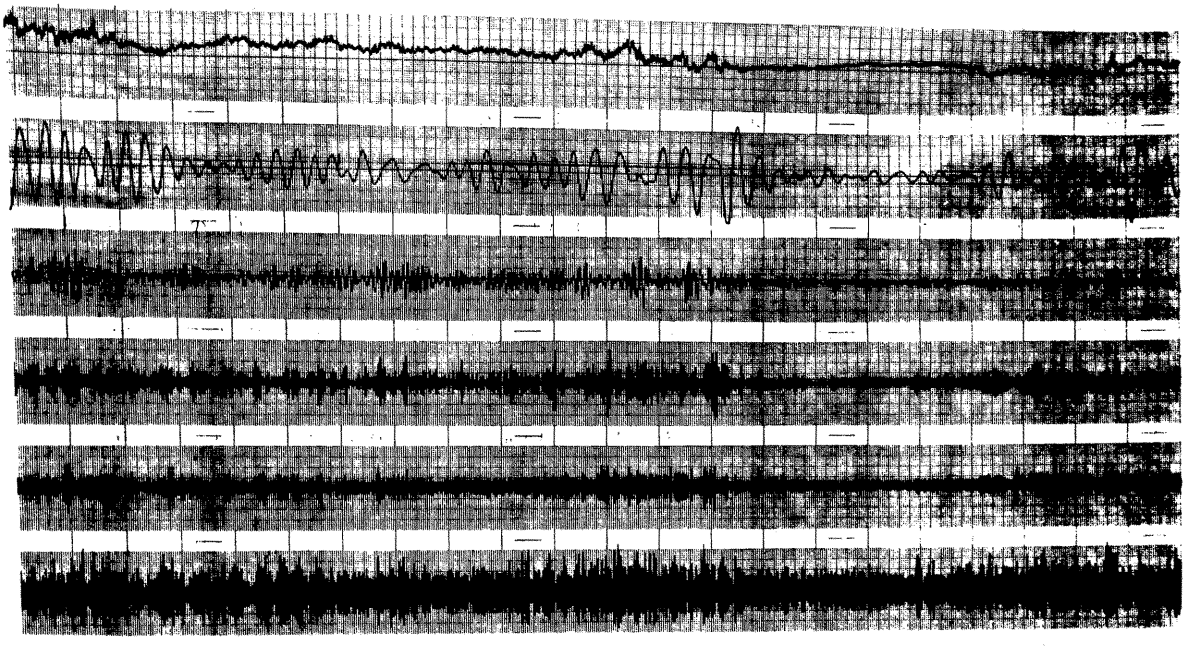

Chart Speed .2 cm/sec

Fig. 10 65 foot level hot-wire signal and the same signal decomposed on the different frequencies

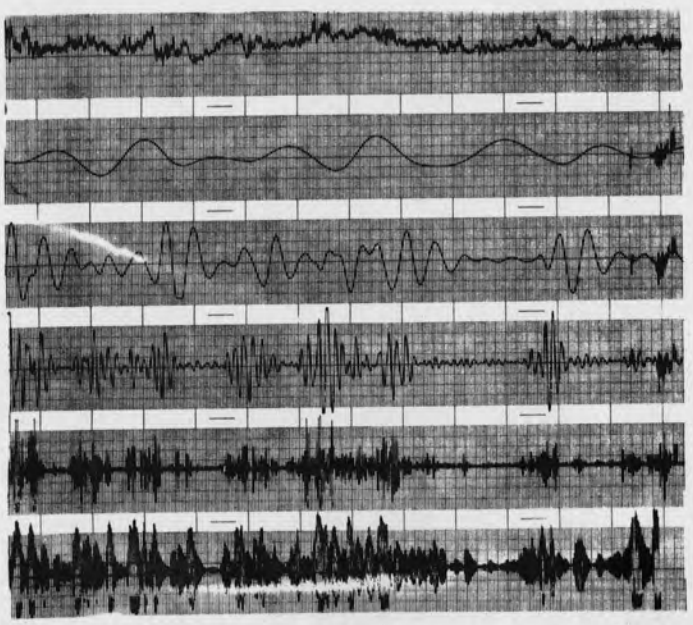

Chart Speed 1 cm/sec

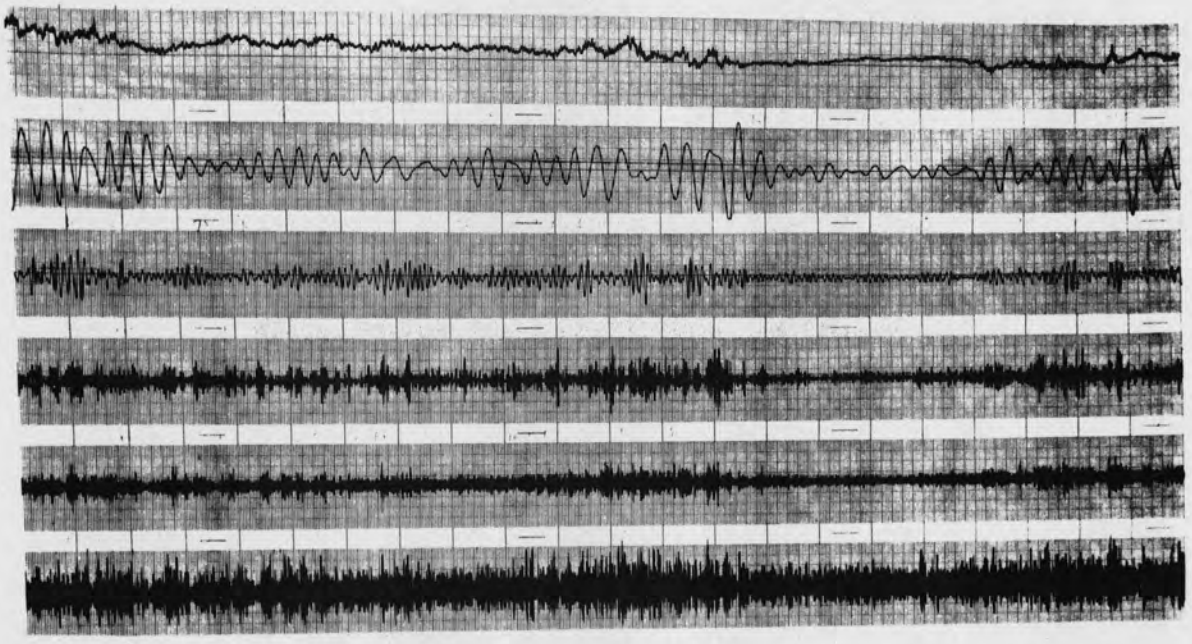

Chart Speed .2 cm/sec

Fig. 10 65 foot level hot-wire signal and the same signal decomposed on the different frequencies

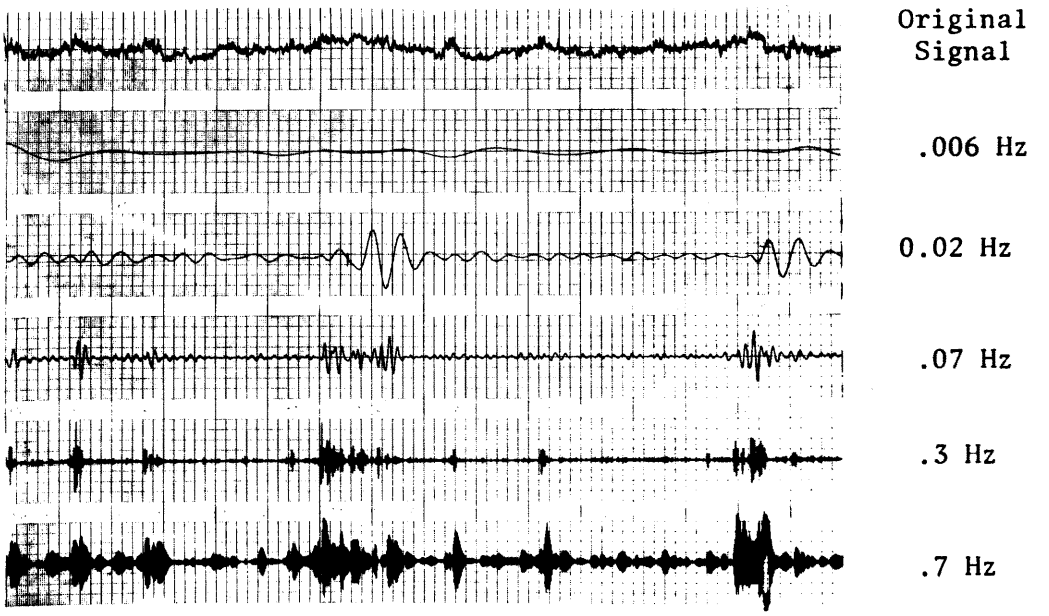

Chart Speed 1 cm/sec

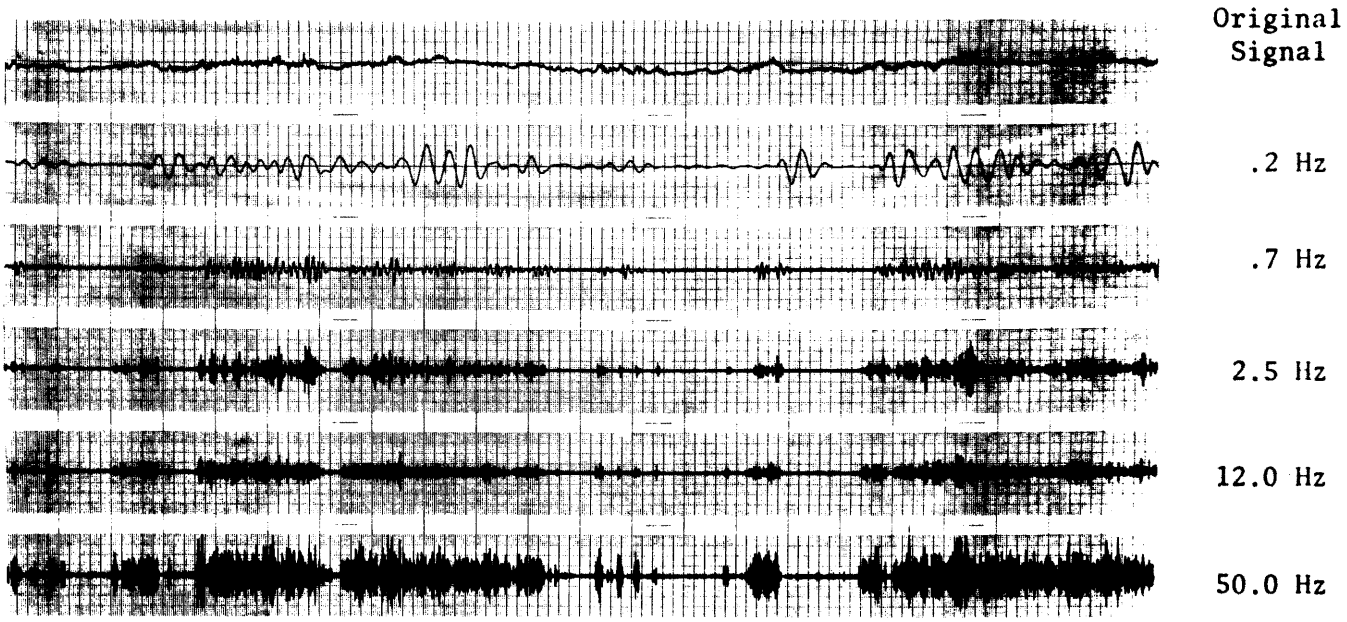

Chart Speed .2 cm/sec

Fig. 11 110 foot level hot-wire signal and the same signal decomposed on the different frequencies

Chart Speed 1 cm/sec

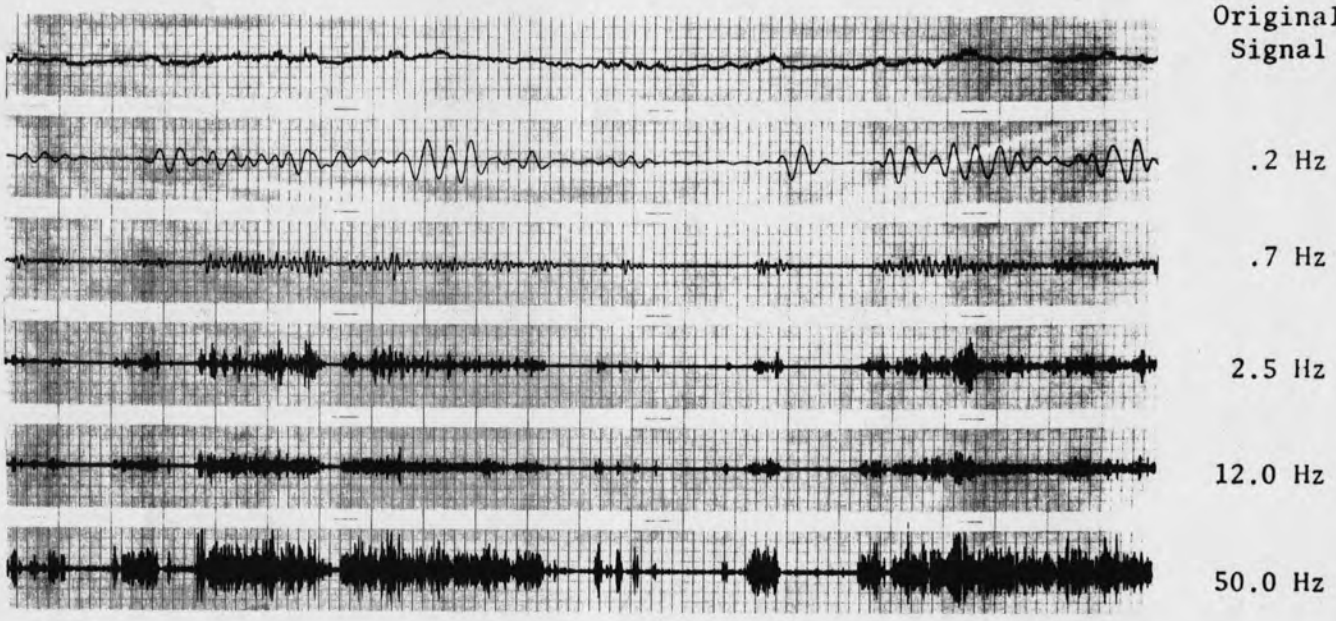

Chart Speed .2 cm/sec

Fig. 11 110 foot level hot-wire signal and the same signal decomposed on the different frequencies

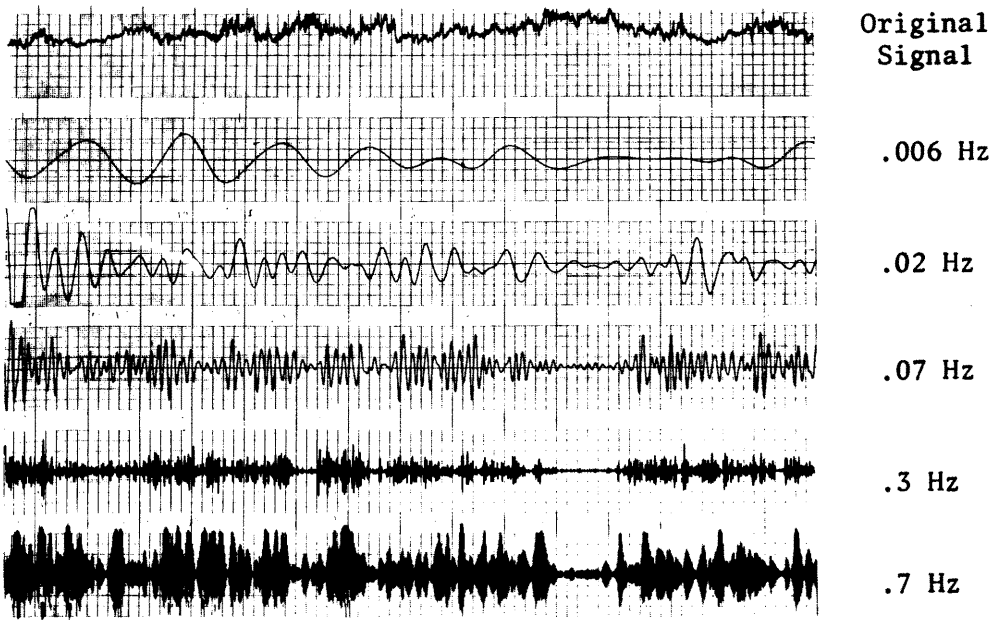

Chart Speed 1 cm/sec

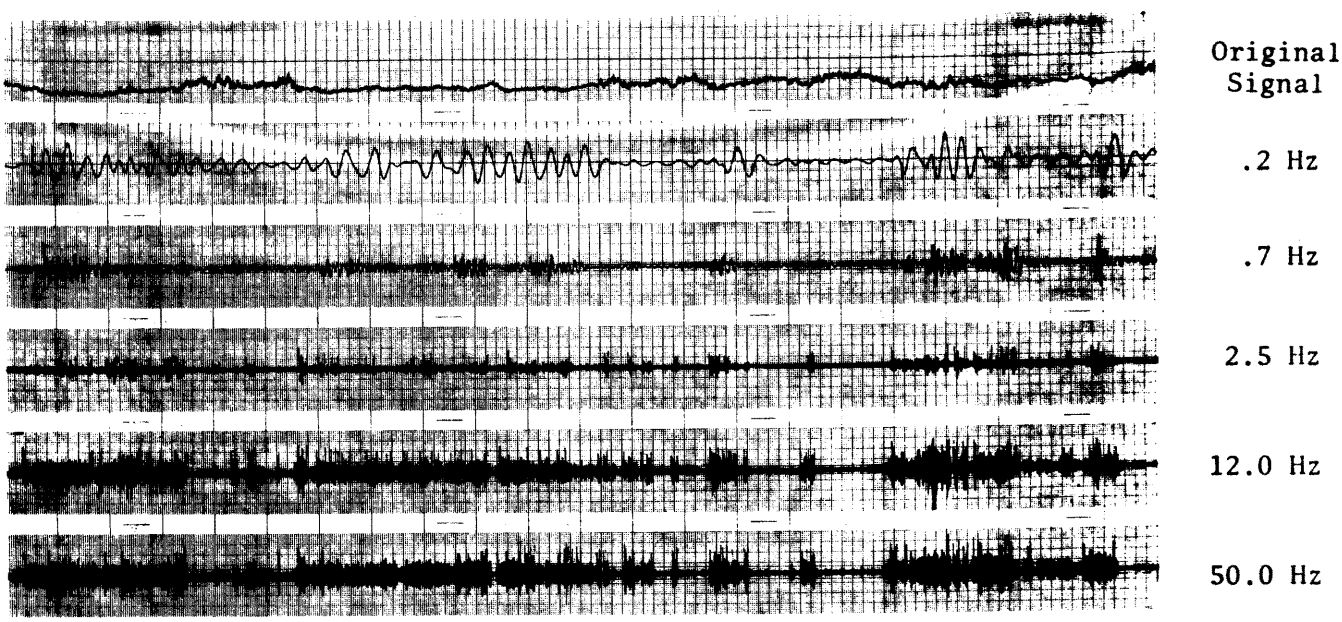

Chart Speed .2 cm/sec

Fig. 12 155 foot level signal and the same signal decomposed on the different frequencies

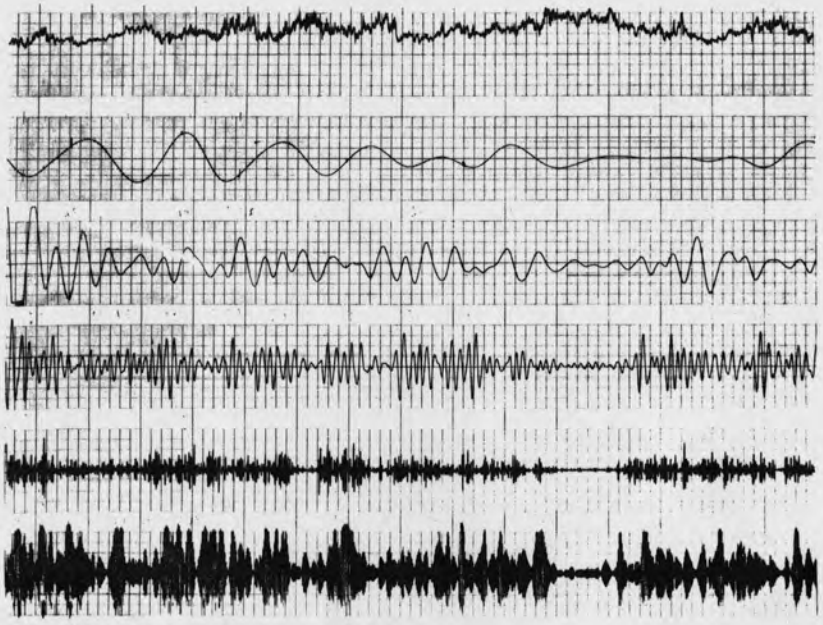

Chart Speed 1 cm/sec

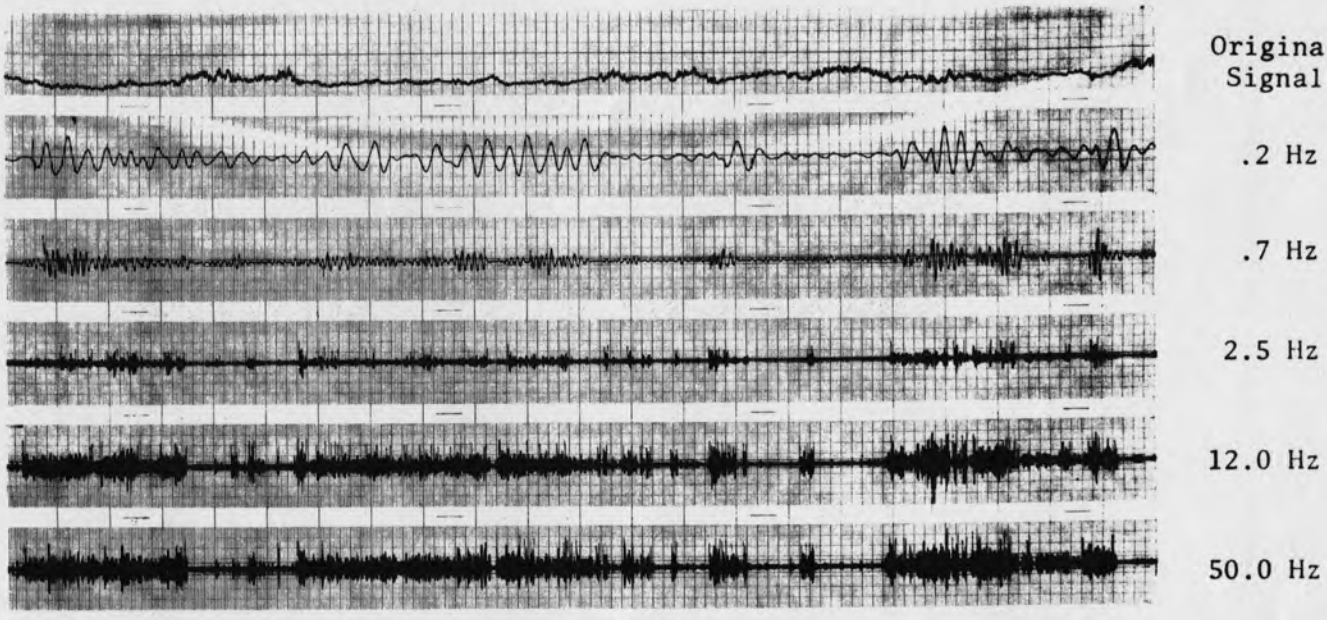

Chart Speed .2 cm/sec

Fig. 12 155 foot level signal and the same signal decomposed on the different frequencies

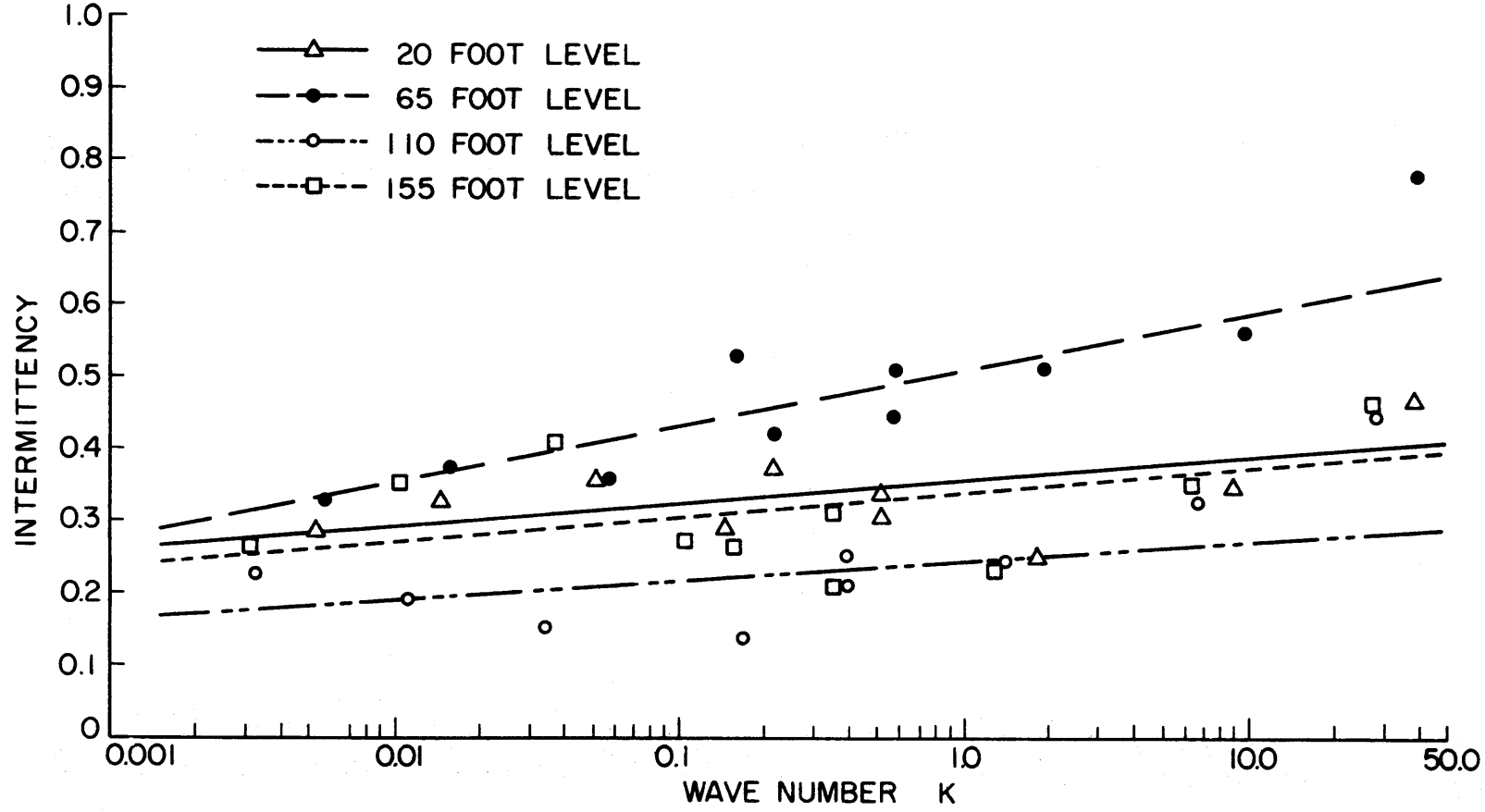

Fig. 13 Intermittency factor γ for different wave numbers at 20 ft, 65 ft, 110 ft, and 155 ft. level.

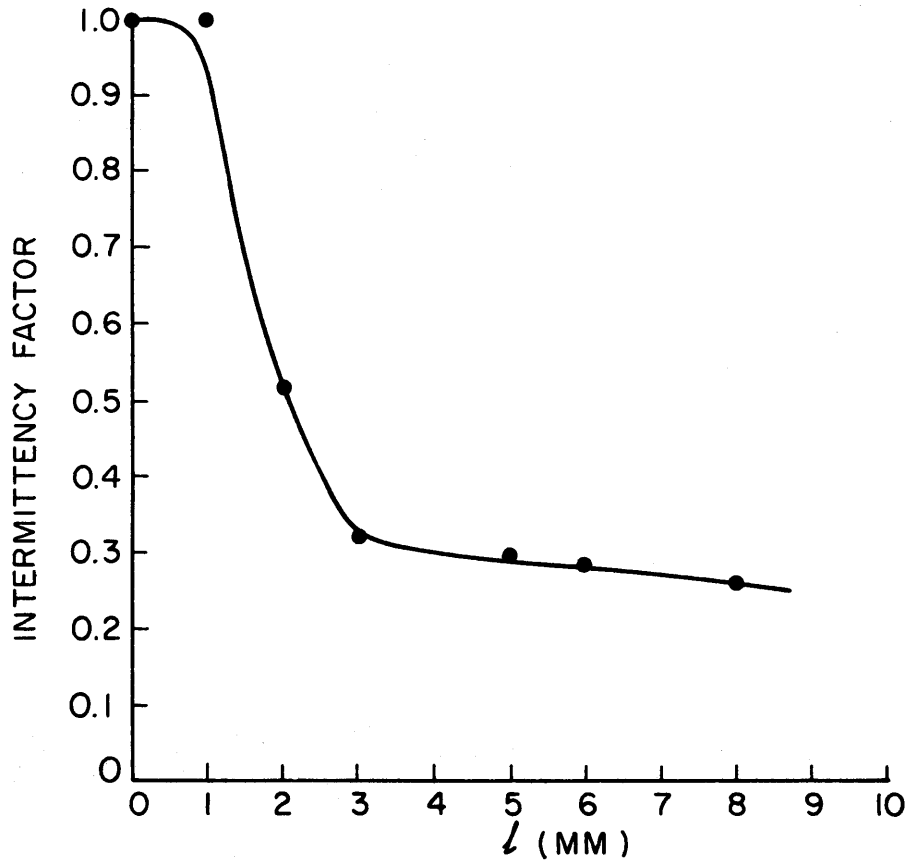

Fig. 14 Intermittency factor γ versus the signal amplitude.

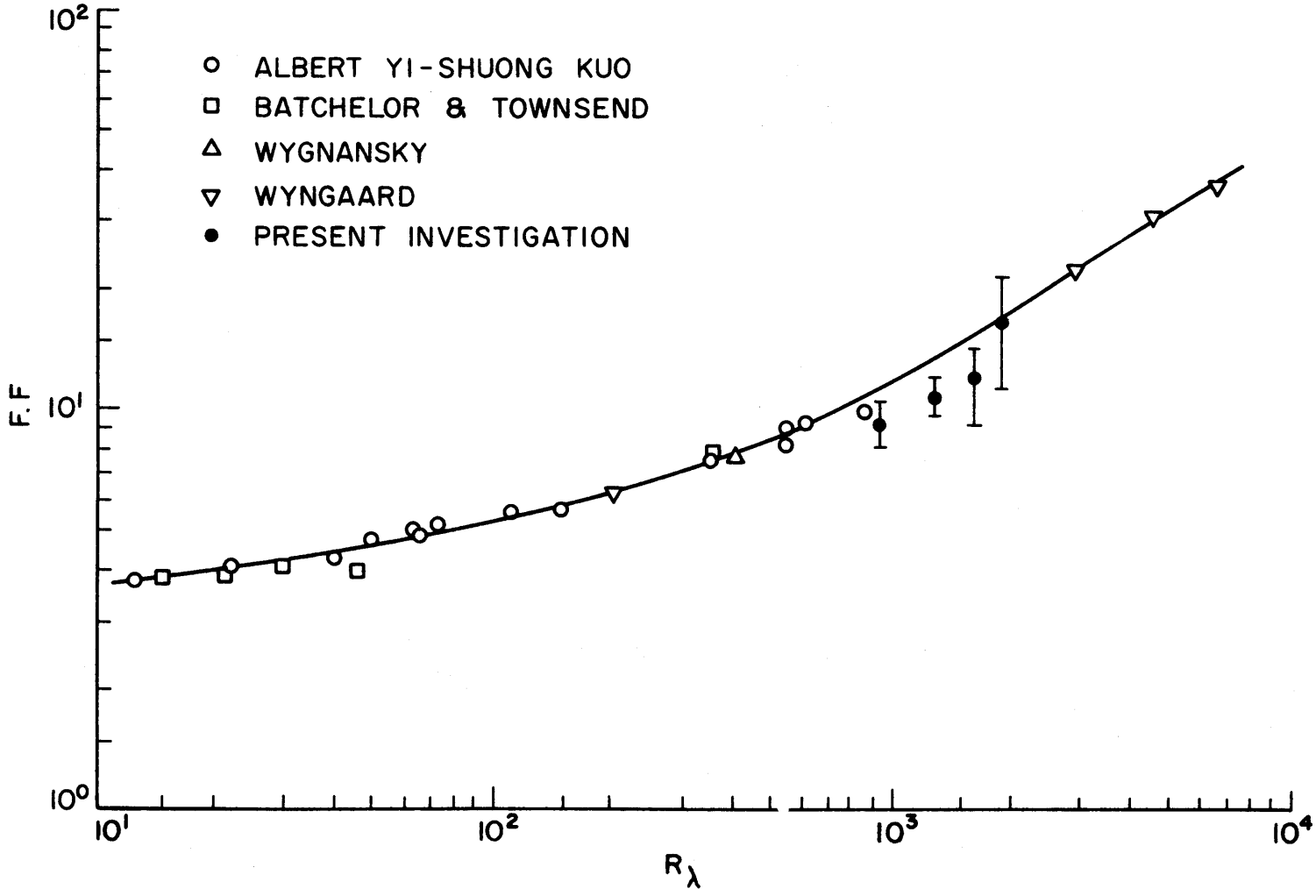

Fig. 15 Flatness factor of $\partial u/\partial t$ as a function of Reynolds number R_λ.

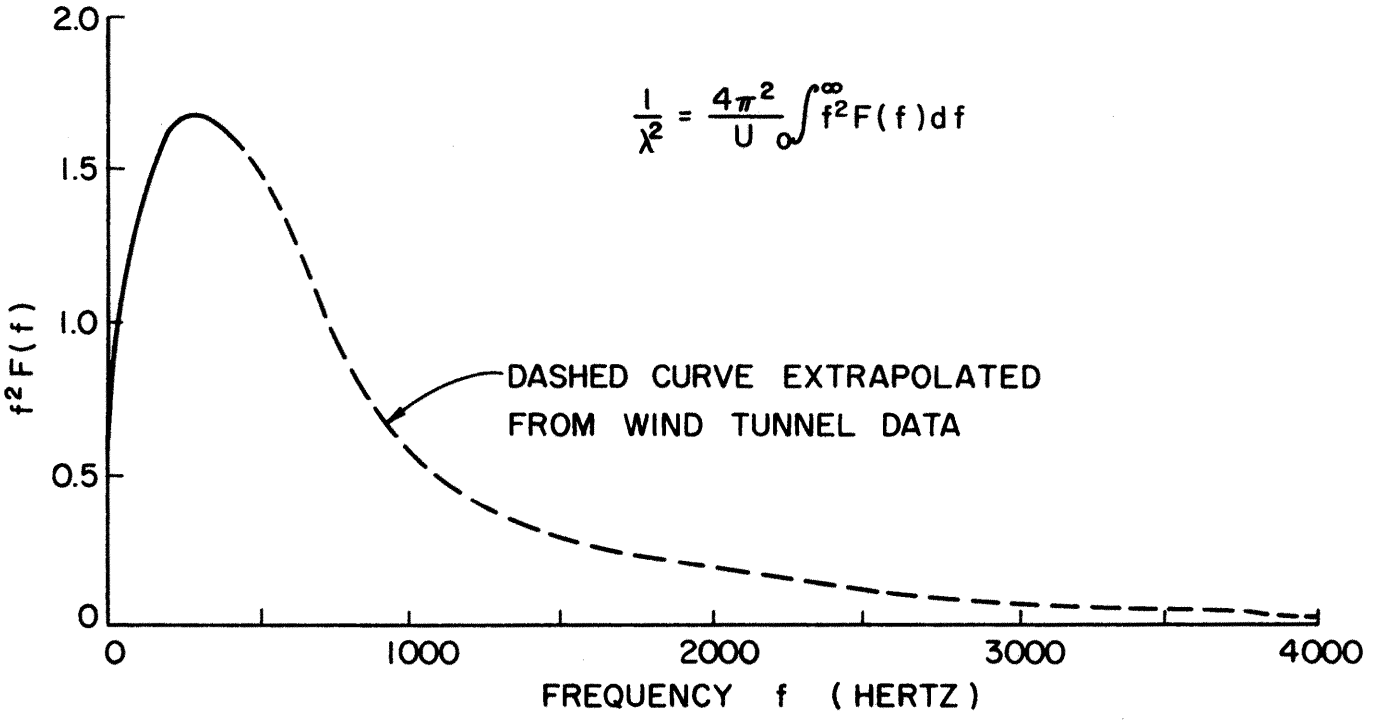

Fig. 16 Second moment of the spectrum curve at a height of 20 feet (G.I. Meters).

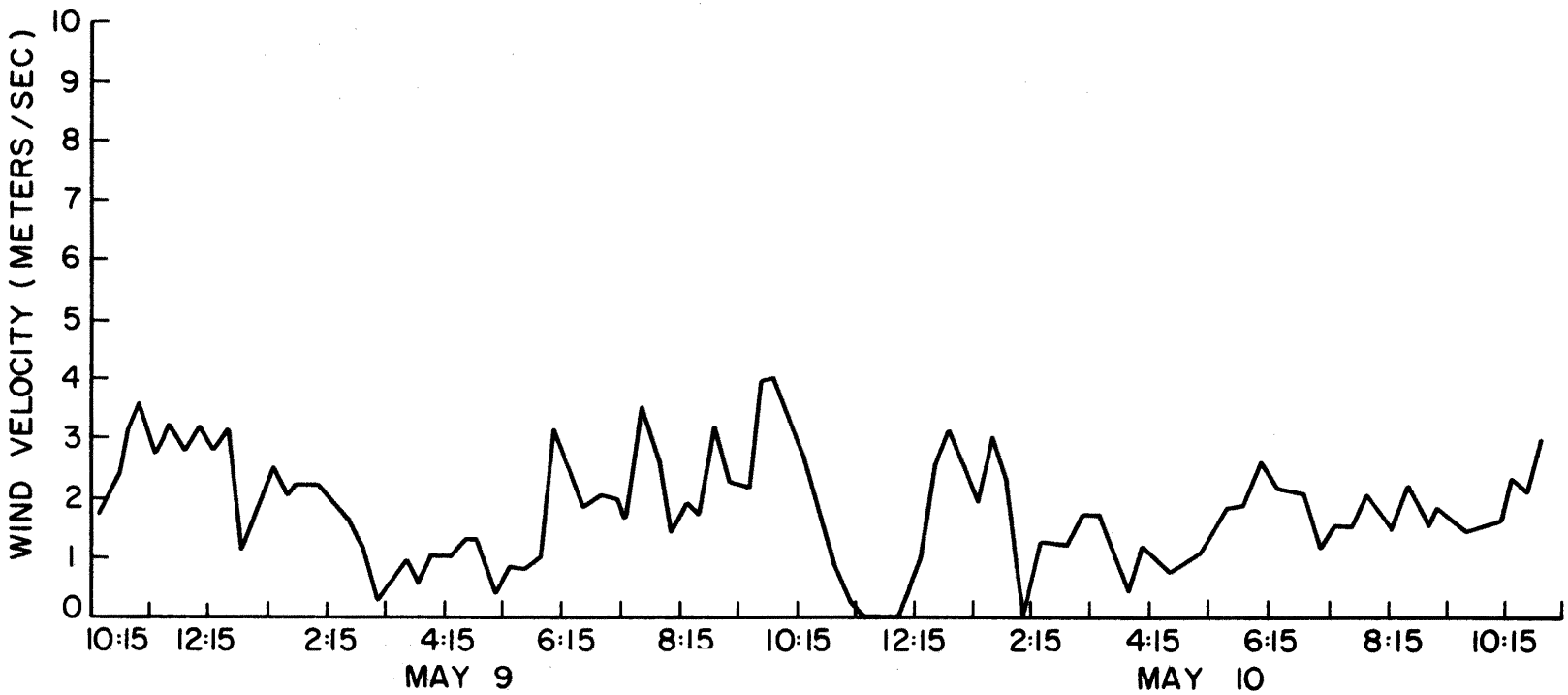

Fig. 17 Mean wind velocity at 10 foot level on May 9, 1968.

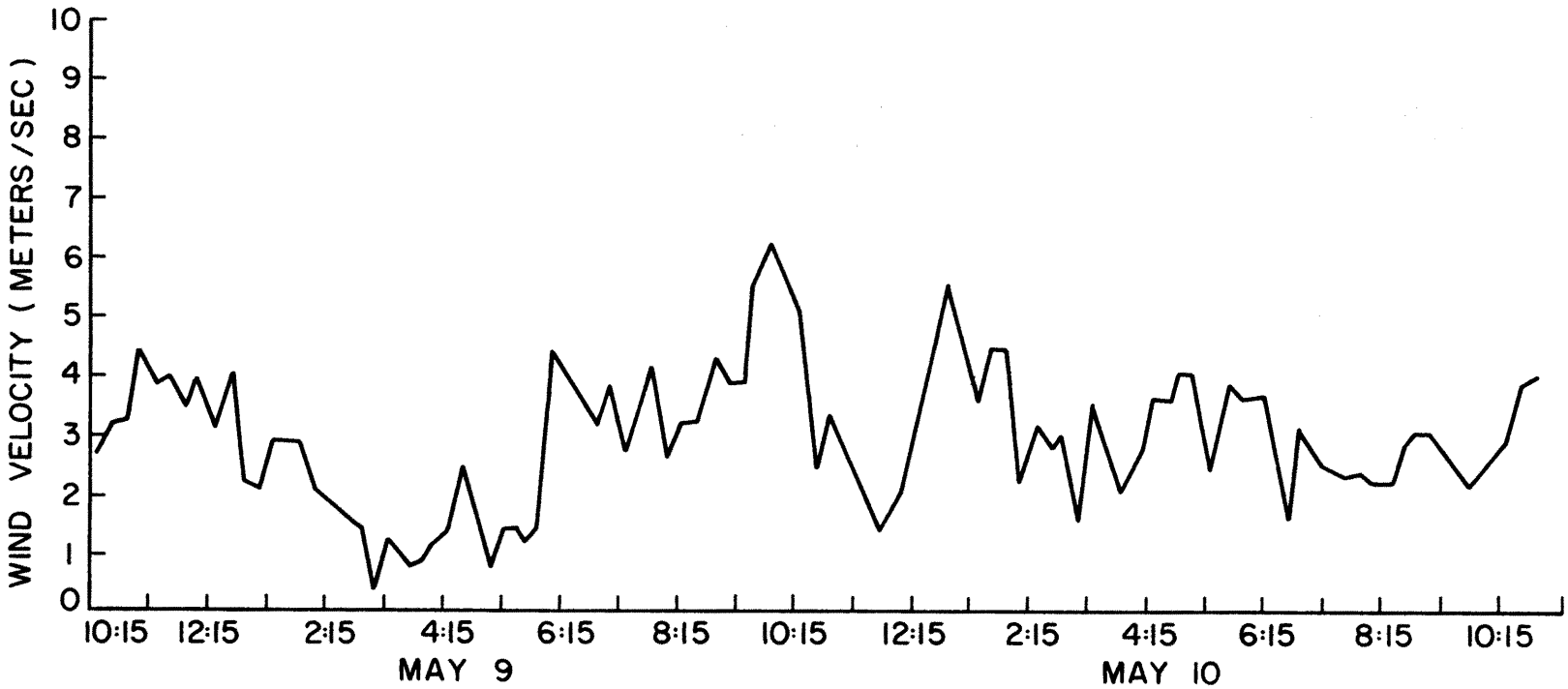

Fig. 18 Mean wind velocity at 110 foot level on May 9, 1968.

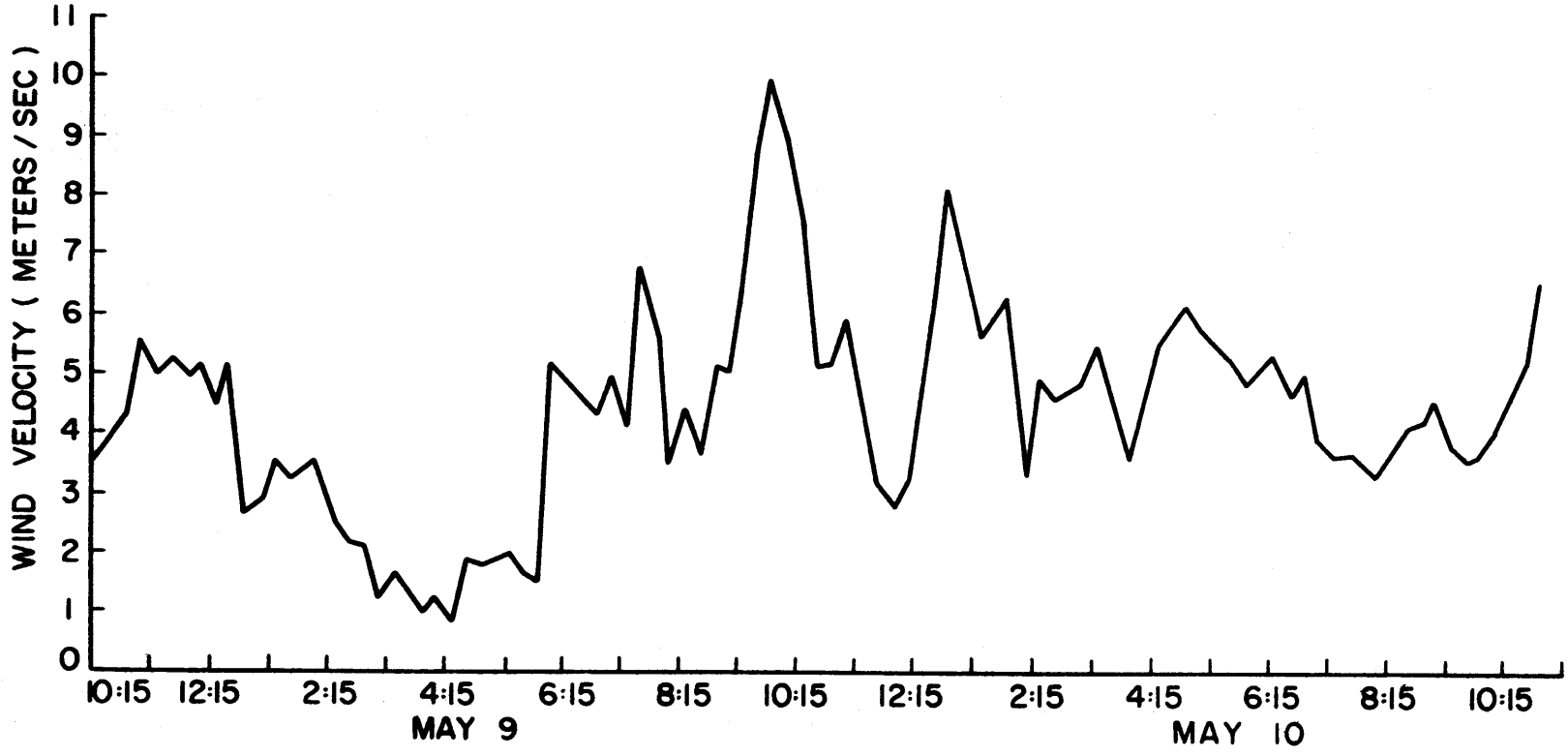

Fig. 19 Mean wind velocity at 200 ft. level on May 9, 1968.

Fig. 20 Temperature variation.

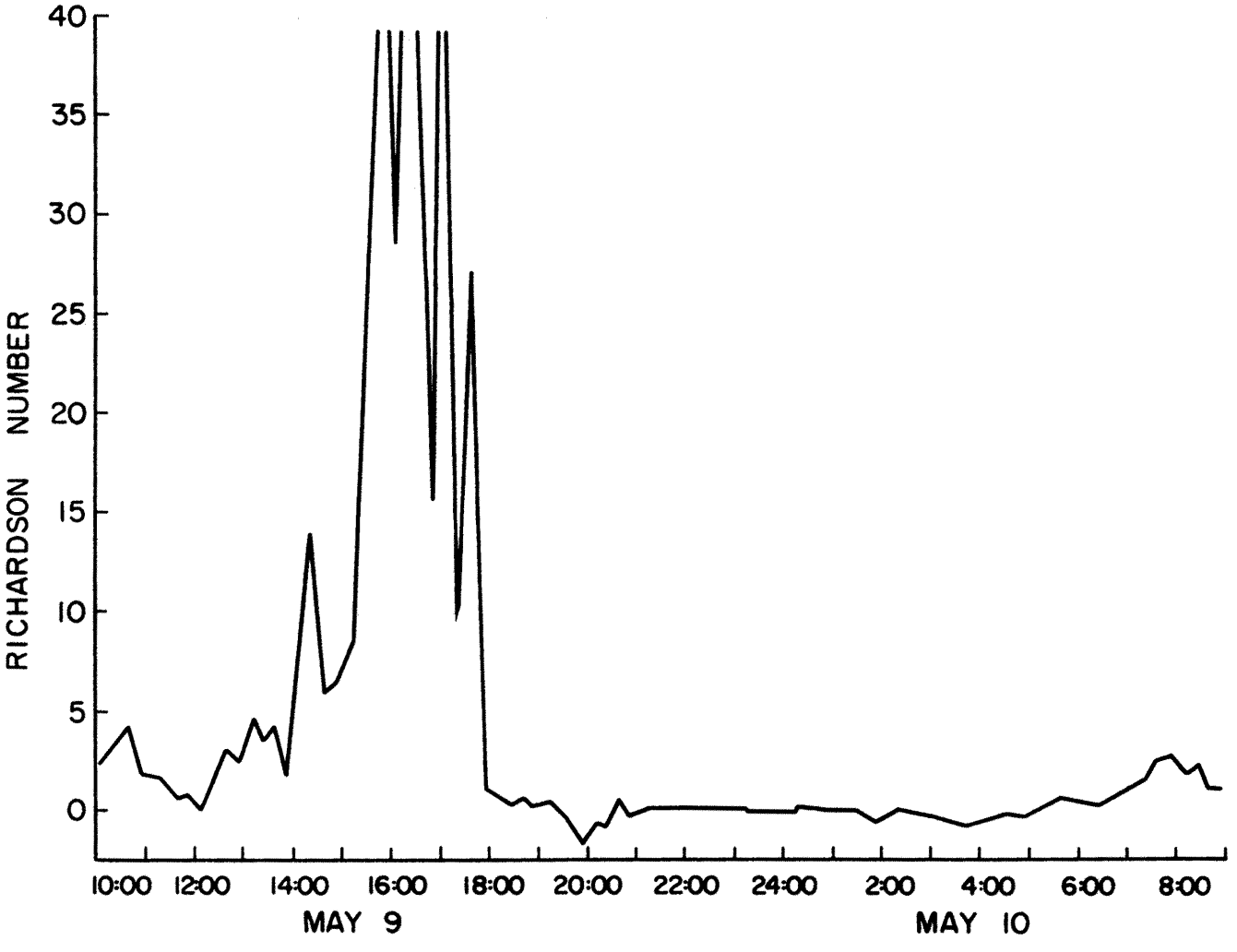

Fig. 21 Variation of Richardson number between 200 and 20 feet.

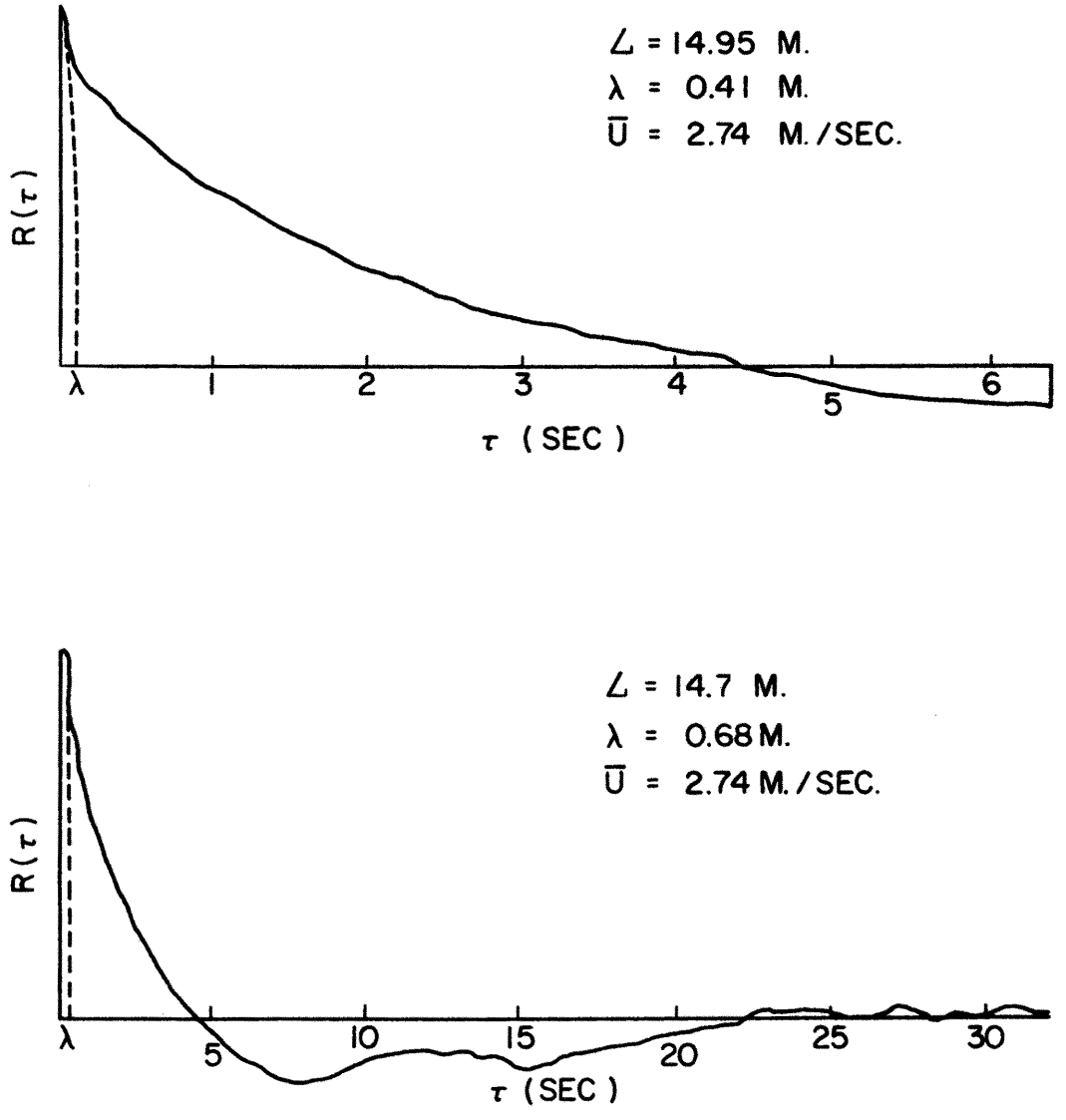

Fig. 22 Autocorrelation functions for hot wire no. 3 at 200 ft. Level on May 9, 1968 at 14:45 - 15:30 P.M.

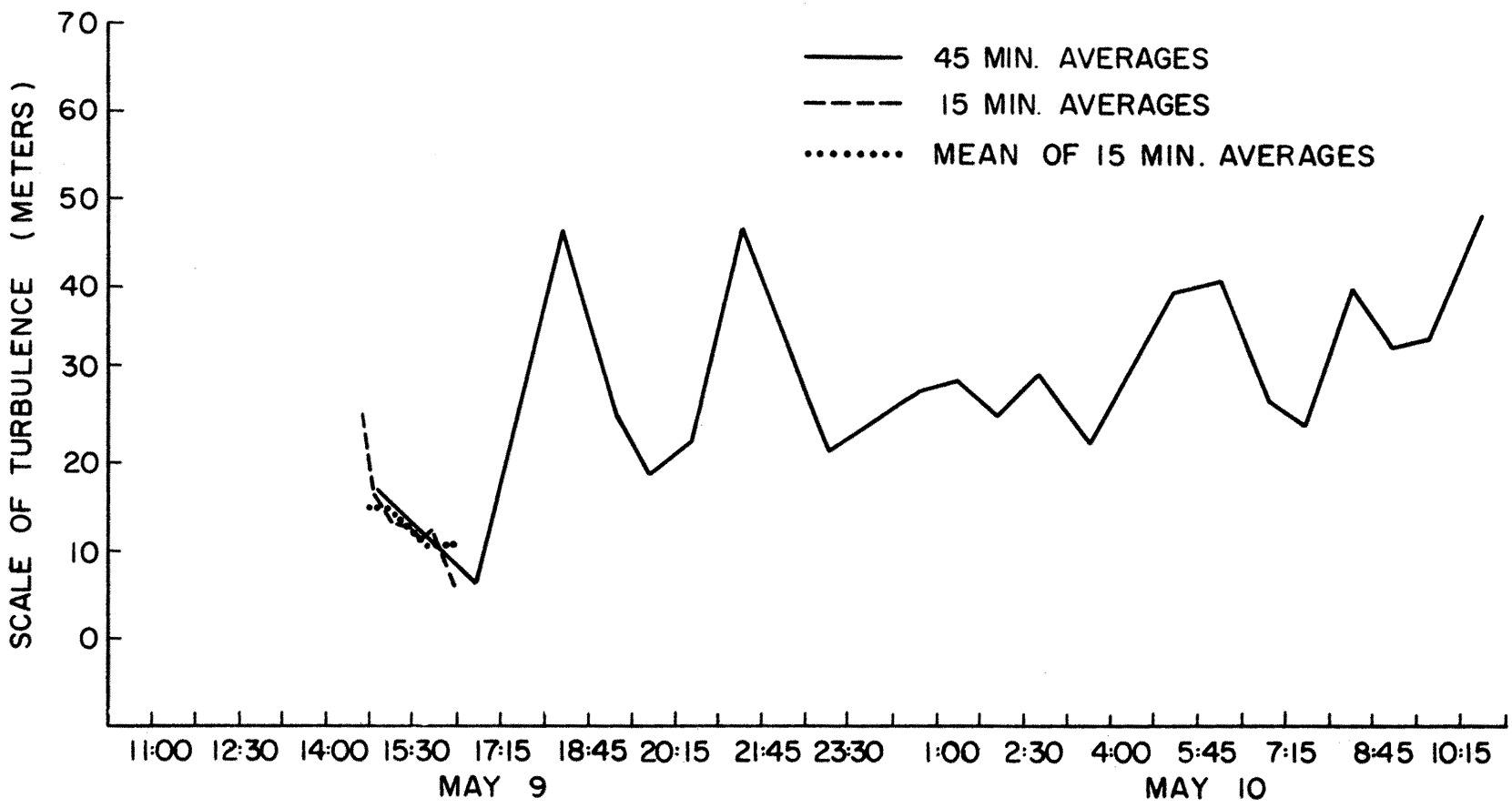

Fig. 23 Scale of turbulence given by hot wire anemometer no 1 on the mast at 200 feet height. Scales calculated by using autocorrelation function.

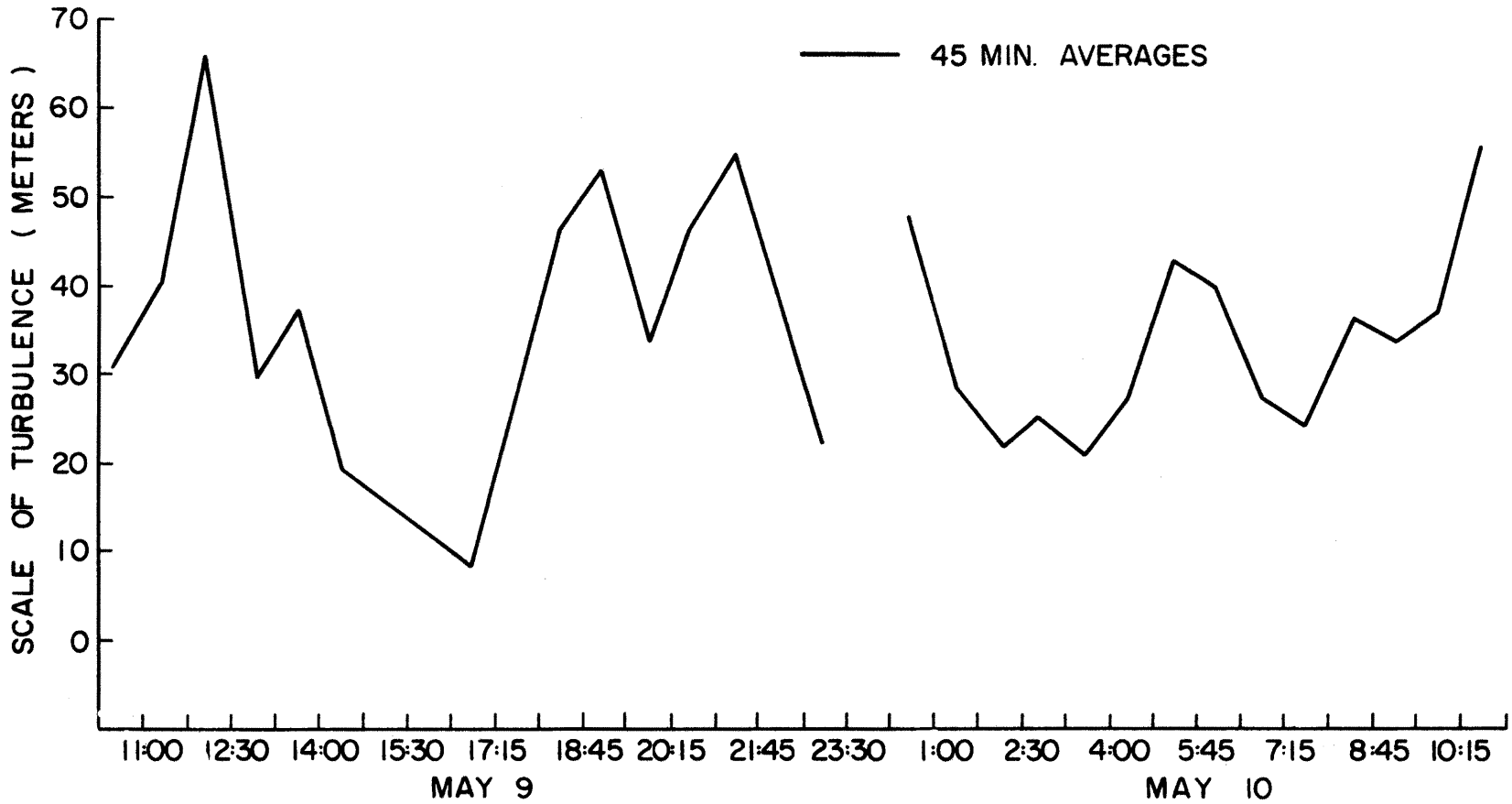

Fig. 24 Scale of turbulence given by hot wire anemometer no. 2 on the mast at 200 feet height. Scales calculated by autocorrelation functions.

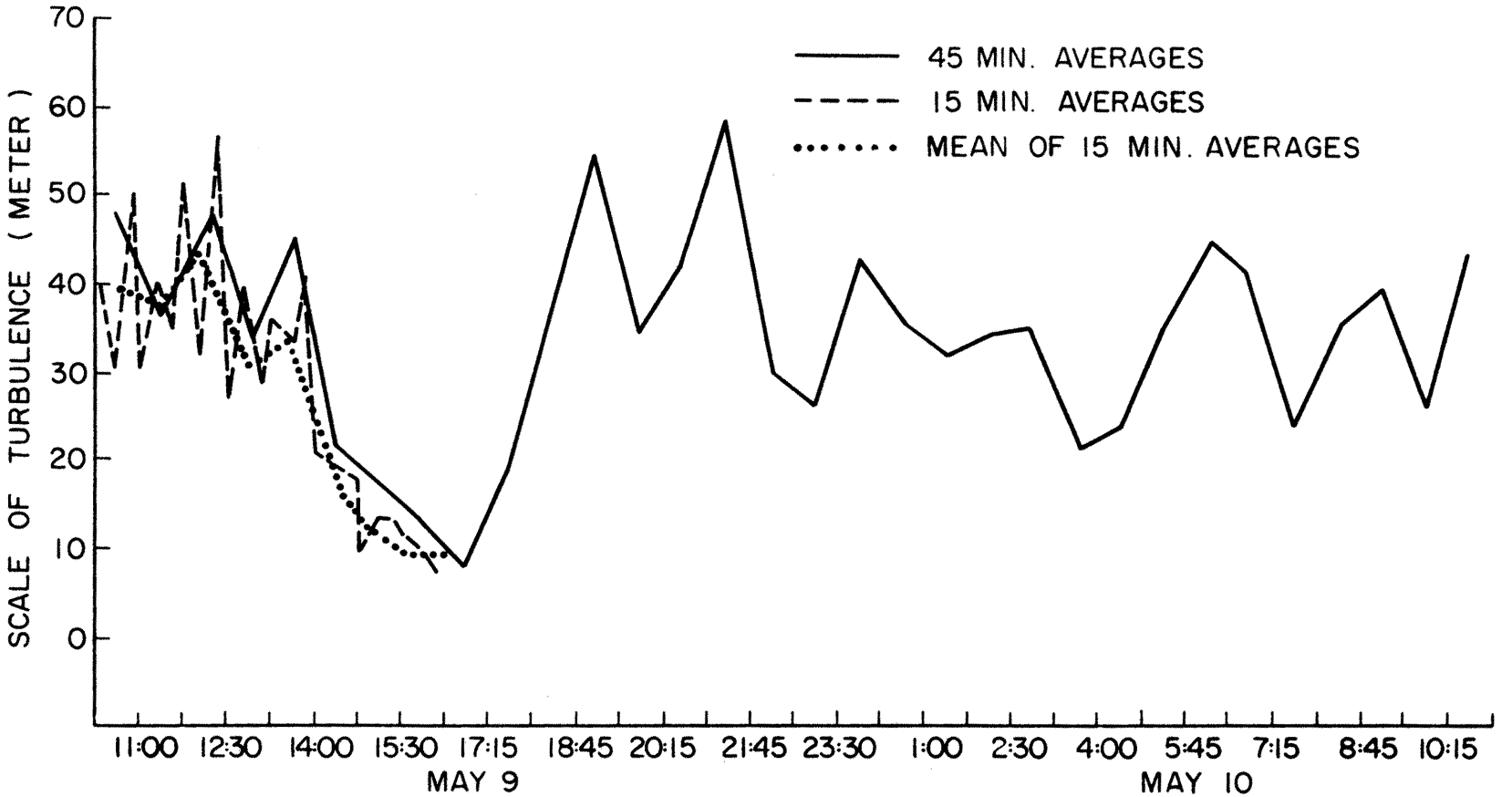

Fig. 25 Scale of turbulence given by hot wire anemometer no. 3 on the mast at 200 feet height. Scales calculated by autocorrelation function.

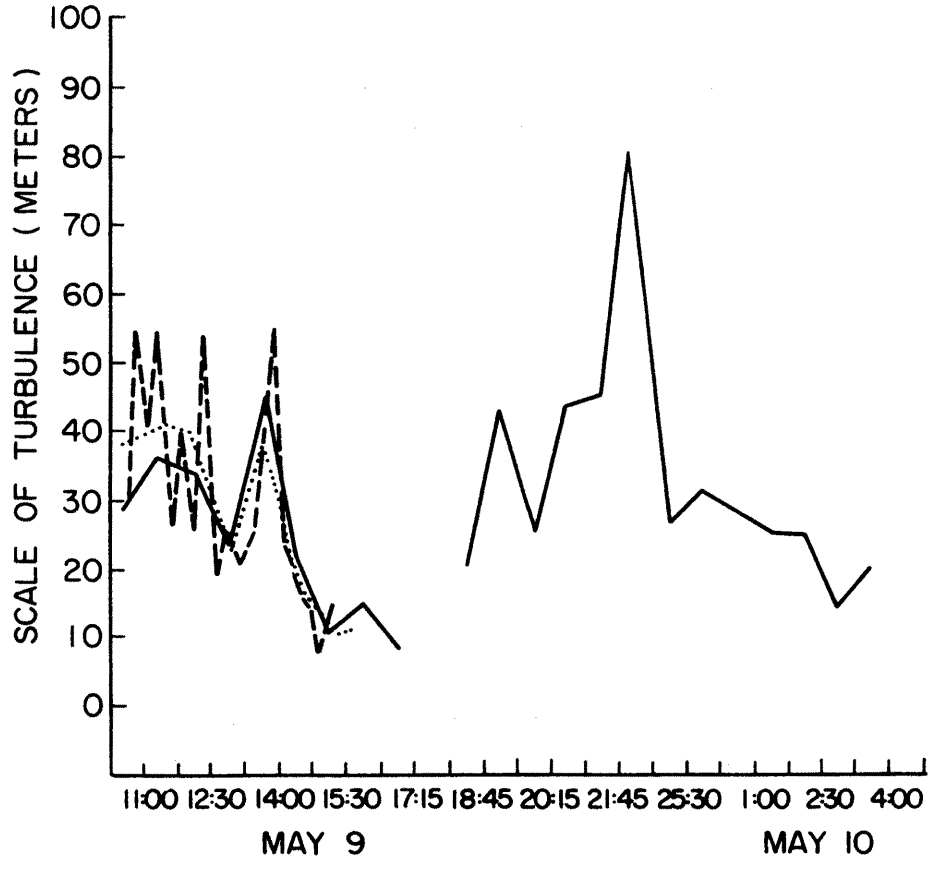

Fig. 26 Scale of turbulence given by hot wire no 4 on the mast at 200 feet height. Scales calculated by autocorrelation functions.

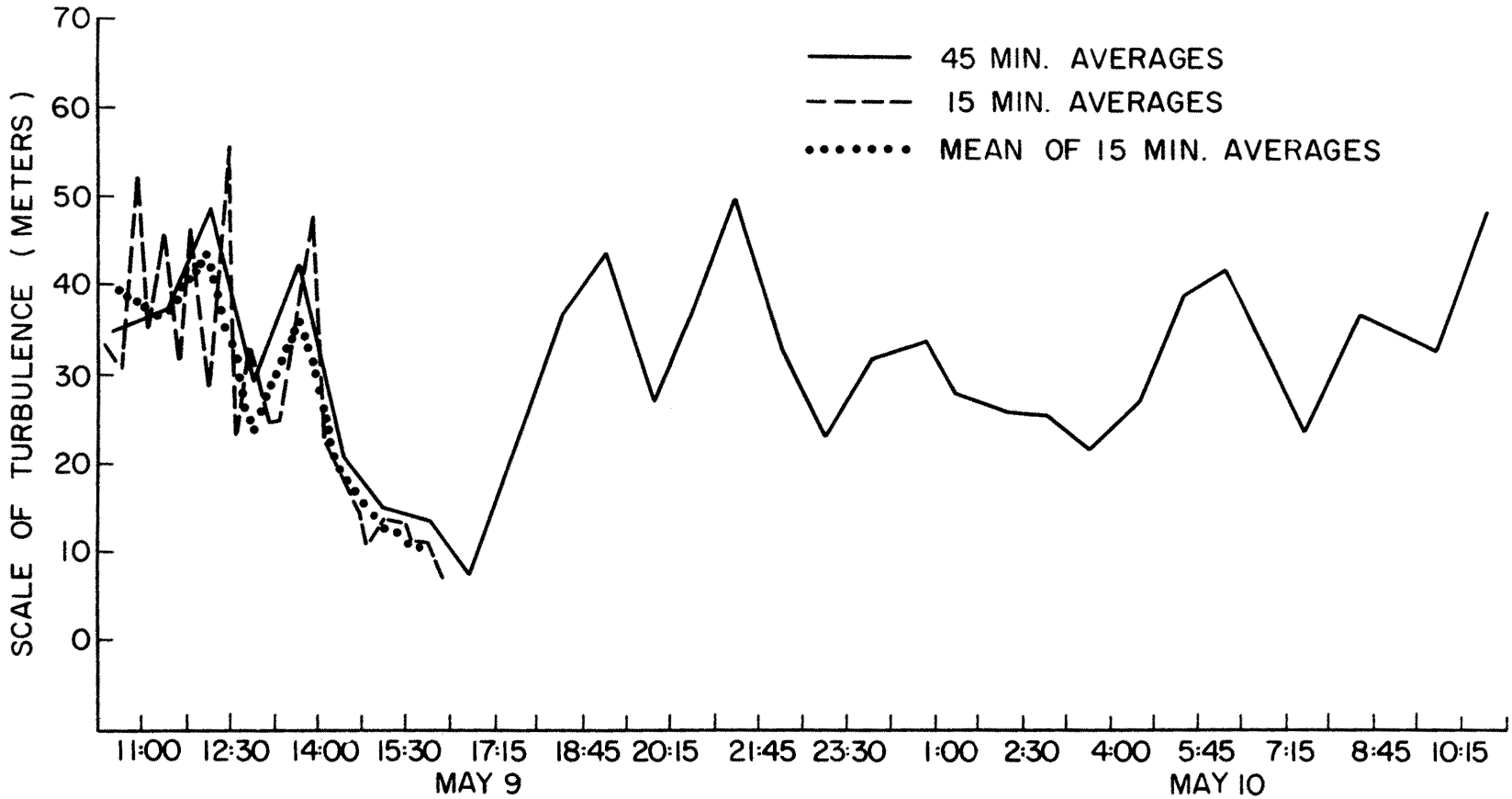

Fig. 27 Scale of turbulence calculated as a mean of four hot wire anemometers at 200 feet height. Scales calculated by autocorrelation functions.

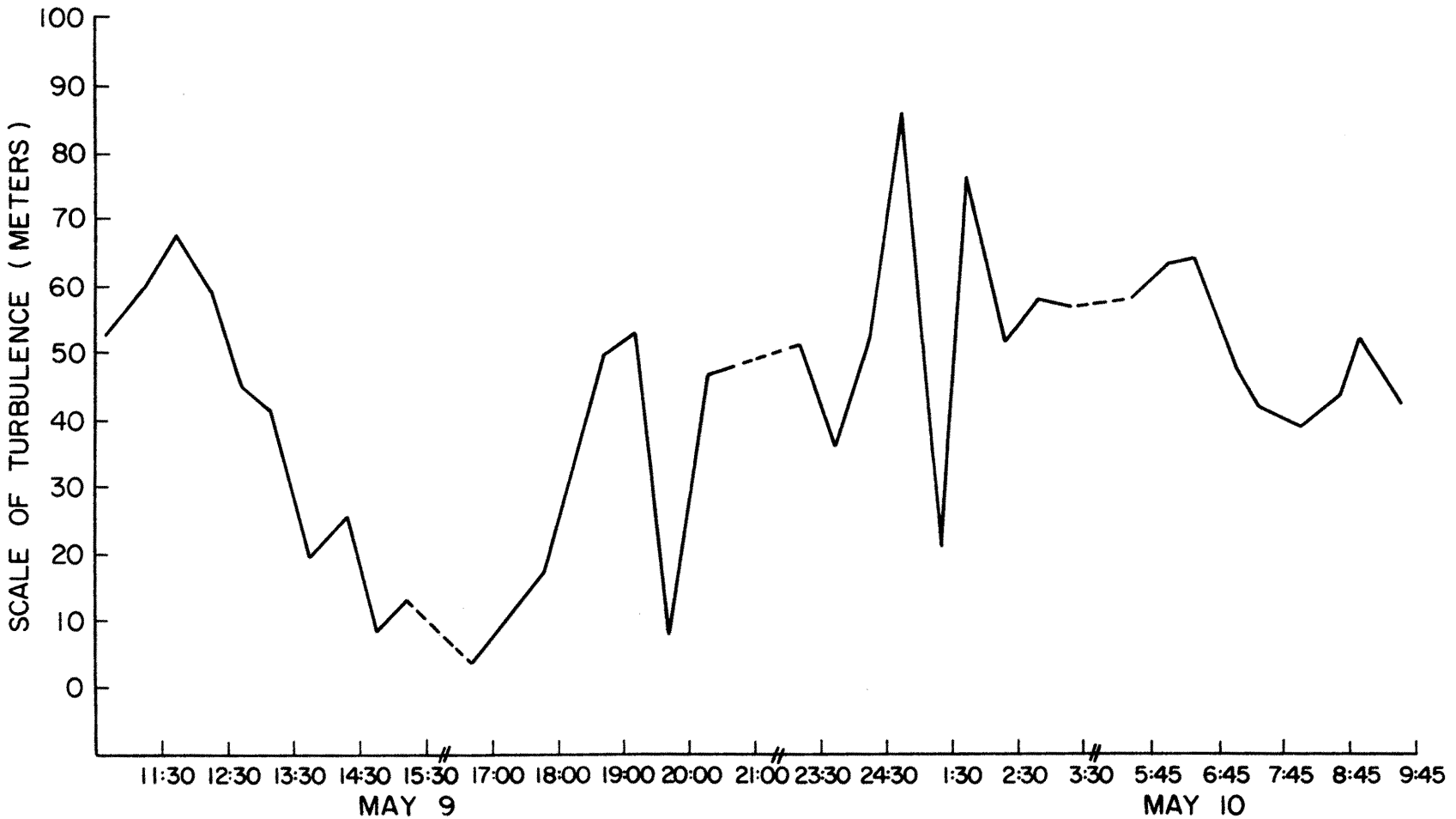

Fig. 28 Scale of turbulence given by hot wire anemometer no. 2.
Scale calculated from spectrum.

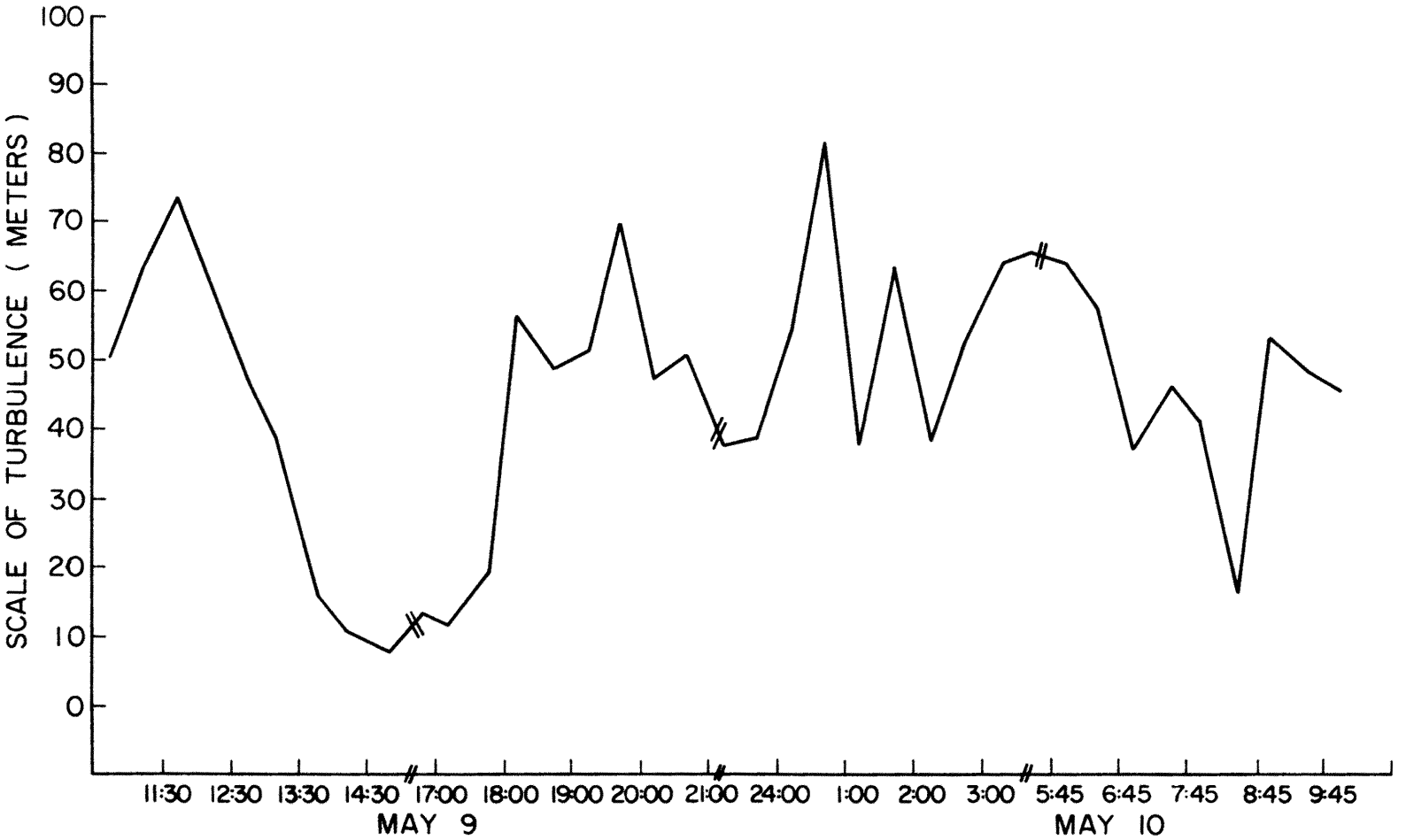

Fig. 29 Scale of turbulence given by hot wire no. 3.
Scale calculated from spectra.